

# CHAPTER 4

## FLOW IN CHANNELS

### INTRODUCTION

**1** Flows in conduits or channels are of interest in science, engineering, and everyday life. Flows in closed conduits or channels, like pipes or air ducts, are entirely in contact with rigid boundaries. Most closed conduits in engineering applications are either circular or rectangular in cross section. *Open-channel flows*, on the other hand, are those whose boundaries are not entirely a solid and rigid material; the other part of the boundary of such flows may be another fluid, or nothing at all. Important open-channel flows are rivers, tidal currents, irrigation canals, or sheets of water running across the ground surface after a rain.

**2** In both closed conduits and open channels, the shape and area of the cross section of the flow can change along the stream; such flows are said to be *nonuniform*. Flows are those that do not change in geometry or flow characteristics from cross section to cross section are said to be *uniform*. Remember that flows can be either *steady* (not changing with time) or *unsteady* (changing with time). In this chapter we will look at laminar and turbulent flows in conduits and channels. The emphasis in this chapter is on steady uniform flow in straight channels. That's a simplification of flows in the natural world, in rivers and in the ocean, but it will reveal many fundamental aspects of those more complicated flows. The material in this chapter is applicable to a much broader class of flows, in pipes and conduits, as well; such matters are covered in standard textbooks on fluid dynamics.

**3** This chapter focuses on two of the most important aspects of channel flow: *boundary resistance to flow*, and the *velocity structure of the flow*. The discussion is built around two reference cases: steady uniform flow in a circular pipe, and steady uniform flow down an inclined plane. Flow in a circular pipe is clearly of great practical and engineering importance, and it is given lots of space in fluid-dynamics textbooks. Flow down a plane is more relevant to natural Earth-surface settings (sheet floods come to mind), and it serves as a good reference for river flows.

**4** The first section looks at laminar flow in a planar open channel, to derive expressions for the distributions of shear stress and velocity across the cross section. There are two equivalent ways of doing that: specializing the Navier–Stokes equations (which, remember, are a general

statement of Newton's second law as applied to fluid flows) to the given kind of flow, or writing Newton's second law directly for the given kind of flow. We will take the second approach here. Then in further sections we will tackle the much more difficult problem of resistance and velocity in turbulent flows in pipes and channels. That will necessitate a deeper examination of the nature of shear stresses in turbulent flow, and a careful consideration of the differences between what I will call smooth flow and rough flow. The outcome will be some widely useful techniques as well as greatly increased understanding. The section on velocity distributions is intricate and lengthy, and may not seem as directly useful, but it reveals some really fundamental concepts.

### LAMINAR FLOW DOWN AN INCLINED PLANE

**5** In this section we apply Newton's second law to steady and uniform flow down an inclined plane. The strategy is to look at a block of the flow, bounded by imaginary planes normal to the bottom, with unit cross-stream width and unit streamwise distance (Figure 4-1). In fluid dynamics, such a block of fluid is said to be a "free body". Because the flow is assumed to be steady and uniform, all of the forces in the streamwise direction that are exerted upon the fluid within the free body at any given time must add up to be zero.

**6** I should mention at the outset that for now I will not address how the flow is arranged so that the flow is uniform. If you just pour a sheet of water onto the plane along some particular horizontal line on the plane, you should not expect that uniform flow will automatically be established downslope of that line in the sense that the flow depth is the same at all normal-to-flow sections farther down the plane, and in general it is not: you would need to adjust the slope of the plane to attain a state of uniformity. This is not a trivial problem, and it should await some more detailed material, later in this chapter, on flow resistance. On the other hand, it should make intuitive sense to you that if the plane is very long the degree of nonuniformity would be very small whatever the slope: just imagine pouring water from a row of little faucets onto a plane a mile long and sloping a few degrees.

**7** Obviously only liquids, not gases, can flow as open-channel flows. The freely deformable upper surface of the liquid, called the *free surface*, is open to the air. We will neglect the minor forces exerted by the overlying air on the moving liquid. Our idealized channel flow is of infinite width, with no side boundaries, and it is therefore just a convenient abstraction. But a flow in a channel of rectangular cross section with the width of flow

much greater than the depth of flow is a good approximation to a flow with infinite width.

**8** Take the  $x$  direction to be downstream and the  $y$  direction to be normal to the boundary, with  $y = 0$  at the bottom of the flow (Figure 4-1). By the no-slip condition, the velocity is zero at  $y = 0$ , so the velocity must increase upward in the flow. It is also clear that the flow is everywhere directed straight down the plane. Think about the forces acting on the fluid contained at a given instant in the free body within the rectangular volume formed by the free surface, the bottom boundary, and two pairs of imaginary planes normal to the bottom and with unit spacing, one pair parallel to the flow and spaced a distance  $B$  apart, and the other normal to the flow and spaced a distance  $L$  apart (Figure 4-1).

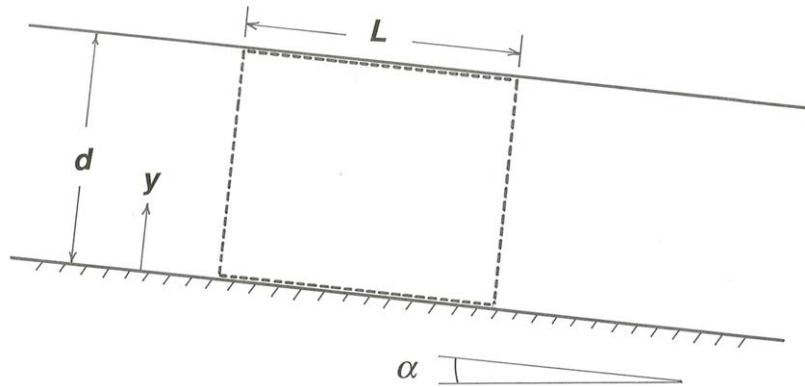


Figure 4-1. Definition sketch for deriving the boundary shear stress in steady uniform flow down an inclined plane.

---

**9** Writing Newton's second law for the balance of forces on this free body means equating the downslope driving force, caused by the downslope component of the weight of the fluid in the free body, with the resistance force exerted by the planar boundary on the lower surface of the free body. The weight of the fluid in the free body is  $\gamma BLd$ , where  $d$  is the depth of flow. The downslope component of this weight is  $\gamma \sin \alpha BLd$ , where  $\alpha$  is the slope angle of the plane (Figure 4-2).

---

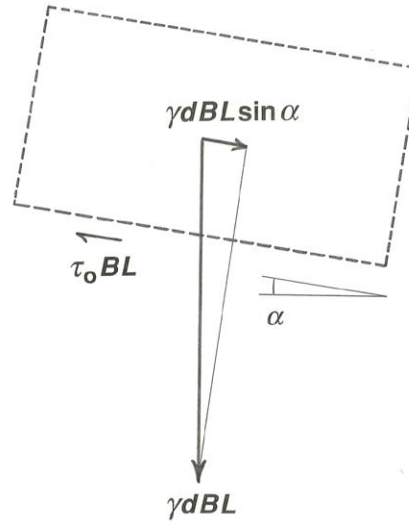


Figure 4-2. Forces on a free body of fluid in steady uniform flow down an inclined plane.

This is balanced by the frictional force  $\tau_0 BL$  exerted by the bottom boundary. There are also pressure forces acting parallel to the flow direction on the upstream and downstream faces of the free body, but because by our assumption of uniformity the vertical distribution of these pressure forces is the same at every cross section, they balance each other out and cause no net force on the free body. Setting  $\gamma \sin \alpha BLd$  equal to  $\tau_0 BL$  and solving for  $\tau_0$ ,

$$\tau_0 = \gamma d \sin \alpha \quad (4.1)$$

so the boundary shear stress is directly proportional to the product of the flow depth, the specific weight of the liquid, and the sine of the slope angle.

**10** Before we continue with the development, we will make the resistance equation more relevant to the real world by writing a similar equation for a channel with rectangular cross section and then for a channel with arbitrary (but unvarying) cross section. To generalize Equation 4.1 to a rectangular channel, take the flow width to be  $b$  (Figure 4-3) and write the force balance for a free body that fills the channel, from wall to wall, in a segment of length  $L$  along the flow. Doing the same mathematics as above gives the result

$$\tau_o = \gamma \sin \alpha \frac{bd}{2d+b} \quad (4.2)$$

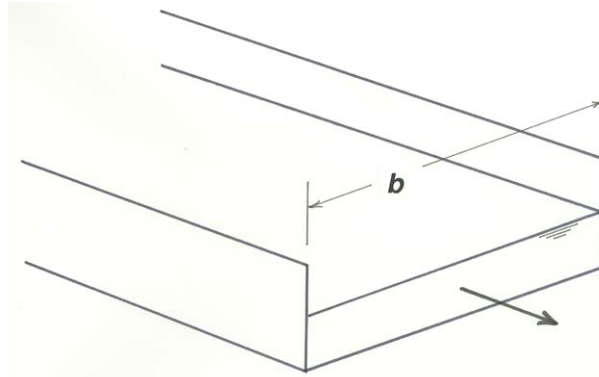


Figure 4-3. Sketch of a rectangular open channel of width  $b$ , to aid in the definition of the hydraulic radius.

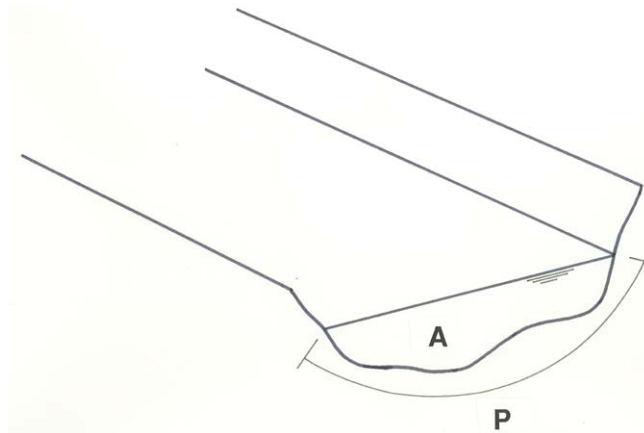


Figure 4-4. The wetted perimeter of a straight open channel flow.

**11** To generalize Equation 4.1 to a channel of arbitrary cross-section shape, assume that the area of the cross section is  $A$  and the wetted perimeter (the distance along the submerged part of the boundary from waterline to waterline) is  $P$  (Figure 4-4). The same balance of forces gives

$$\tau_o = \gamma \sin \alpha \frac{A}{P} \quad (4.3)$$

**12** Equations 4.1, 4.2, and 4.3 look rather different, but they can easily be unified by defining a quantity called the *hydraulic radius*  $R_H$  formed by dividing the cross-sectional area of the flow by the wetted perimeter. You can verify for yourself that the hydraulic radius of flow in a rectangular channel is  $bd/(2d+b)$ . It is a little more difficult to see that the hydraulic radius of an infinitely wide channel flow is just the flow depth  $d$ . You can reason that as the width  $b$  increases relative to the depth  $d$ , the term  $2d$  in the denominator  $2d+b$  becomes a smaller and smaller part of the denominator, so the hydraulic radius  $bd/(2d+b)$  tends toward  $bd/b$ , or just  $d$ , as the width increases relative to the depth. The right-hand sides of all three equations, 4.1, 4.2, and 4.3, become  $\gamma \sin\alpha R_H$ .

**13** Equation 4.3, or its special cases Equation 4.1 or Equation 4.2, is the basic resistance equation for steady uniform flow in an open channel. Not many useful results in fluid mechanics are so easily derived! It is the principal way that the boundary shear stress is found in rivers (although to use it that way you need to do some surveying to establish the elevation of the water surface at two points along the channel, at least hundreds if not thousands of meters apart). Sometimes the three equations are written in terms of the slope,  $\tan\alpha$ , rather than the sine of the slope angle,  $\sin\alpha$ , because for very small  $\alpha$  (the usual case), the approximation  $\sin\alpha \approx \tan\alpha$  is a good one.

**14** Now back to the infinitely wide flow down a plane: now that you know how to find the boundary shear stress, what can be said about how the shear stress and flow velocity within the flow vary with height above the bottom? One thing you already know for sure: by the no-slip condition, *the velocity at the very bottom must be zero*. Another thing you can say without further derivation is that *the velocity must be at its maximum at the free surface*. Why? Because the downslope driving force of gravity is a “body force” that acts throughout the flow, whereas resisting friction force acts only at the bottom. The flow velocity must therefore increase monotonically upward in the flow.

**15** We can find the shear stress and velocity at all points up in the flow by applying the same force-balancing procedure to a free body of fluid similar to that used above but with its lower face formed by an imaginary plane a variable distance  $y$  above the bottom and parallel to it (Figure 4-5). The shear stress  $\tau$  across the plane is given directly by the force balance:

---

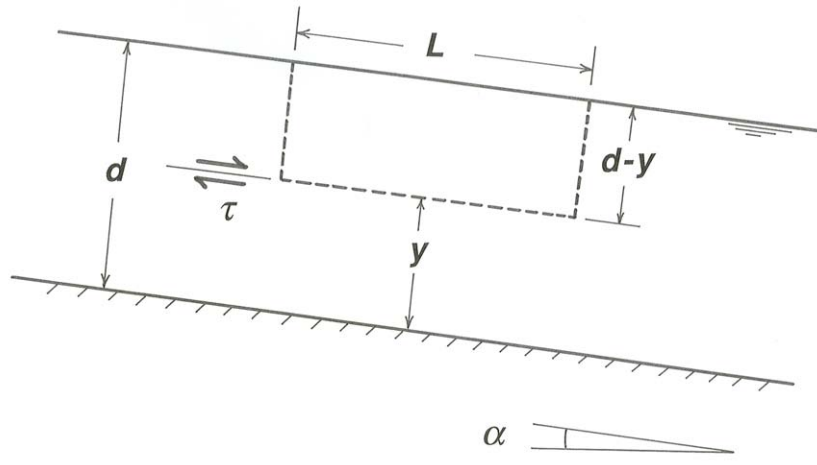


Figure 4-5. Definition sketch for deriving the distribution of shear stress in steady uniform laminar open-channel flow.

---


$$\tau = \gamma \sin \alpha (d-y) \tag{4.4}$$

Using Equation 4.1 to eliminate  $\gamma \sin \alpha$  from Equation 4.4, we can write  $\tau$  in terms of the boundary shear stress  $\tau_0$ :

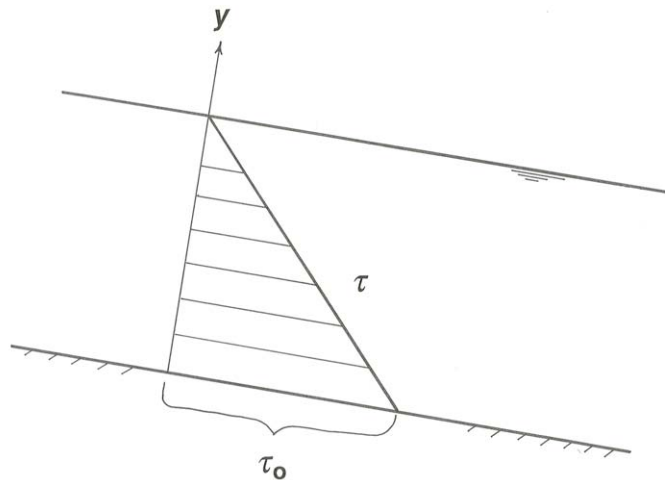


Figure 4-6. The distribution of shear stress in steady uniform laminar open-channel flow. (It is noted later in the text that this distribution holds for turbulent flow as well.)

$$\tau = \tau_o \left( 1 - \frac{y}{d} \right) \quad (4.5)$$

Equation 4.5 shows that  $\tau$  varies linearly from a maximum of  $\gamma \sin \alpha$  at the bottom to zero at the surface (Figure 4-6).

**16** Eliminating  $\tau$  from Equation 4.4 by use of Equation 1.8 gives an expression for the velocity gradient  $du/dy$ :

$$\begin{aligned} \mu \frac{du}{dy} &= \gamma \sin \alpha (d-y) \\ \frac{du}{dy} &= \frac{\gamma \sin \alpha}{\mu} (d-y) \end{aligned} \quad (4.6)$$

Equation 4.6 can be integrated to give the velocity distribution from the bottom boundary to the free surface:

$$\begin{aligned} u &= \int \frac{du}{dy} dy \\ &= \int \frac{\gamma \sin \alpha}{\mu} (d-y) dy \\ &= \frac{\gamma \sin \alpha}{\mu} (d \int dy + \int y dy) \\ &= \frac{\gamma \sin \alpha}{\mu} \left( yd + \frac{1}{2}y^2 \right) + c \end{aligned}$$

We can evaluate the constant of integration  $c$  by use of the boundary condition that  $u = 0$  at  $y = 0$ ; we find that  $c = 0$ , so

$$u = \frac{\gamma \sin \alpha}{\mu} \left( yd + \frac{1}{2}y^2 \right) \quad (4.7)$$

**17** For given values of  $\gamma$ ,  $\alpha$ ,  $\mu$ , and  $d$ , the velocity  $u$  thus varies *parabolically* from zero at the bottom boundary to a maximum at the surface (Figure 4-7). On the other hand, from Equation 4.7 the velocity gradient  $du/dy$  varies linearly from a maximum at the bottom to zero at the free surface, because it is directly proportional to the shear stress (Figure 4-7).

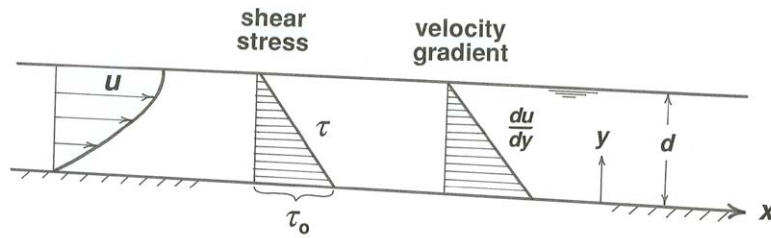


Figure 4-7. The vertical distribution of velocity, shear stress, and velocity gradient in steady uniform laminar open-channel flow.

**18** Here is a reminder about shearing within a flowing fluid, which you first encountered back in Chapter 1. You can think, loosely, in terms of layers of the fluid sliding past one another. A good way of making that concrete is to obtain a very thick telephone book and “rack” its pages by putting your hands firmly on the front and back covers and sliding them parallel to one another in the direction perpendicular to the spine of the book. In fluids, of course, the shearing is continuous rather than in the form of discrete layers.

### TURBULENT FLOW IN CHANNELS: INITIAL MATERIAL

**19** The big question at this point is this: how applicable to real flows are the equations for the distribution of shear stress and velocity in steady uniform flows in circular pipes and open channels derived in the preceding section? If you made experiments with pipe flows and channel flows at very low Reynolds numbers, before the transition to turbulent flow (remember, this would necessitate combinations of low velocities, high viscosities, and small flow depths and diameters), you would find beautiful agreement between theory and observation—something that is always satisfying for both the theoretician and the experimentalist. But for turbulent flows, which is the situation in most flows that are of practical interest, the story is different.

**20** Figure 4-8 shows a comparison of velocity profiles, in both pipes and channels, between laminar and turbulent flows arranged to have the same discharge. It is clear that the turbulent-flow velocity profiles are much more nearly uniform over most of the flow but show a much sharper change in velocity near the boundary, where by the no-slip condition the velocity has to go to zero. It is easy to understand qualitatively why this is so: the exchange of turbulent eddies—macroscopic masses or parcels of fluid—across the surfaces of mean shearing normal to the solid boundaries

is much better at ironing out cross-flow velocity differences than is just the exchange of molecules over short distances in laminar flow. But then the velocity gradient near the boundary, where the normal-to-boundary motions of eddies are inhibited by the presence of the boundary itself, must be even sharper than in laminar flow.

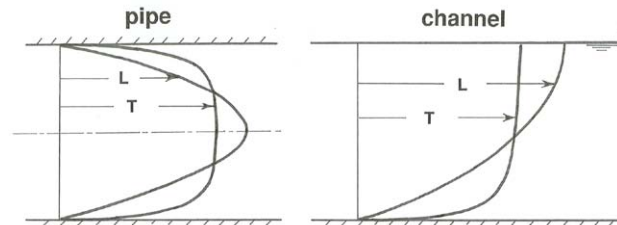


Figure 4-8. Comparison of laminar and turbulent velocity profiles in steady uniform flow in **A)** a circular pipe and **B)** an open-channel flow.

**21** The story with shear stress is different. If you look back at the derivation of Equation 4.4 for the shear-stress distribution in a channel flow, there is nothing in the underlying assumptions that is specific to laminar flow, so the results—the linear distribution of shear stress—should hold just as well in turbulent flow as in laminar flow. I will be making use of that fact later in this chapter.

**22** You might be tempted to ask why Equation 4.7 breaks down for turbulent flow. The most straightforward answer (although not the most important) is, with reference to the channel flow, that we can no longer assume that the shear stress across planes in the flow parallel to the bottom boundary is given by Equation 1.8,  $\tau = \mu(du/dy)$ , so we can no longer eliminate  $\tau$  and perform the integration as in Equation 4.7.

**23** Now to get down to more important reasons: part of the reason Equation 4.7 is no longer applicable is simply that on account of the irregularity of the fluid motion in the turbulent case the surfaces of local shear are oriented differently at each point on such a plane, and the rate or intensity of shear varies as well. But there is a more important reason that has to do with the basic nature of shear stress in turbulent flow past a solid boundary, which I will deal with in the next section. Suffice it to say here that in one important sense the viscosity is effectively much greater in turbulent flows, again because of the efficacy with which turbulent eddies transport fluid momentum across planes of mean shearing; remember that

the basic nature of viscosity itself arises from such momentum exchange on the part of the constituent molecules of the fluid.

**24** This inability to obtain a theoretical velocity distribution in turbulent flows is just one example of a general problem with such flows: it is not possible to solve the equations of motion to obtain exact solutions. The reason for this is basically similar to, although more general than, the problem with velocity profiles noted above: we know what equations we have to solve but we cannot solve them because of the uncertainty that turbulence introduces into the application of these equations. The great number of equations to be found in textbooks and papers on turbulent flow are *semi-empirical*: the general form of the equation may be suggested by physical reasoning, but the numerical constants in the equation, and therefore its specific form, must be found from experiments. And in many cases not even the general form of the equation is known, and the curve must be obtained entirely by experiment. This should become abundantly clear in the material on resistance and velocity profiles in turbulent flow below.

### TURBULENT SHEAR STRESS

**25** One of the most significant effects of turbulence is the transport of such things as heat, momentum, solute, or suspended matter—material or properties that can be viewed as carried passively by the fluid—across planes parallel to the mean flow by the random motions of fluid masses back and forth across these planes. The mean normal-to-boundary velocity across such planes is by definition zero, so the net mass of fluid transferred back and forth in this way must balance to zero on the average. But if the material or property passively associated with the fluid is on the average unevenly distributed—if its average value varies in a direction normal to the mean motion—then the balanced turbulent transfer of fluid across the planes causes a diffusive transport or “flow” of this property, usually referred to as a *flux*, in the direction of decreasing average value. This kind of transport is called *turbulent diffusion*.

**26** To see the turbulent diffusion of some material or property carried by the fluid, think about the result of an exchange of two fluid parcels or eddies with equal mass across a plane of mean shear parallel to the boundary in a turbulent boundary layer (Figure 4-9). The eddy traveling from the side of the plane with higher average value of some property  $P$  tends to arrive on the other side with a higher value of  $P$  than its new surroundings, and conversely the eddy traveling from the side with lower average value tends to arrive with a lower value than its surroundings. The

exchange thus tends to even out the distribution of P by means of a net transport of P in the direction of decreasing average value.

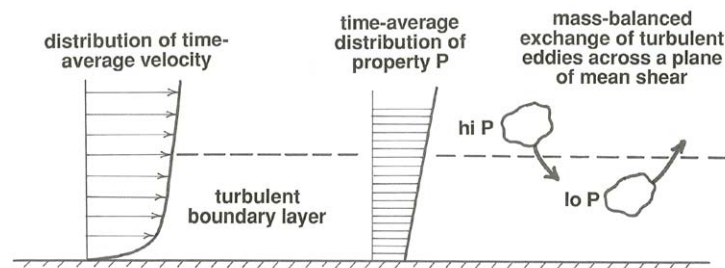


Figure 4-9. Transport of a material or a property by turbulent diffusion in a turbulent boundary layer.

---

**27** An irregular or nonuniform distribution of the property P at the scale of individual eddies is to be expected by the very nature of the diffusion process. So not every eddy that crosses the plane of mean shear shown in Figure 4-9 from the side with higher average P arrives on the other side with a value of P higher than the new surroundings, and conversely not every eddy crossing in the other direction arrives with a lower value of P. But the important point is that there is a *tendency* for this to happen because there is a statistical correlation between values of P and position normal to the plane, and therefore an average gradient of P in that direction. That average gradient is maintained by some process unrelated to diffusion.

**28** A simple but important example is that of sediment carried in suspension by a river or a tidal current or the atmosphere. (We will look at this problem in more detail in Part II.) You know that if a fluid flow is strong enough it can pick up particles of sand or dust from the lower boundary of the flow and carry them high up into the flow, whence they eventually settle back to the bed or the ground. The concentration of the suspended sediment decreases upward, because of the tendency of the sediment to settle through its surrounding fluid. There is a balance between downward settling and upward turbulent diffusion along the concentration gradient (Figure 4-10). The correlation between suspended-sediment concentration and distance above the bottom is clear in Figure 4-10.

---

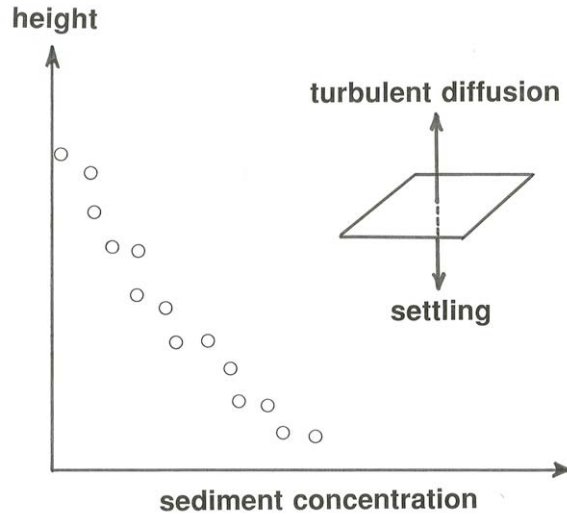


Figure 4-10. Balance between upward transport of suspended sediment by turbulent diffusion and downward transport by settling.

**29** We can appeal to the idea of diffusion of fluid momentum to account for the differences in velocity distribution in laminar and turbulent flow down an inclined plane, discussed in an earlier section of this chapter. In laminar flow there are no eddies to be exchanged across shear planes parallel to the bottom, but the molecules themselves hurtle or weave randomly back and forth across these planes in loose analogy with the picture outlined above for the random motions of turbulent eddies. Because on average the molecules have a greater downchannel velocity in the region above a given shear plane than below it, molecular exchange across the plane tends to even out the distribution of fluid momentum and therefore also of fluid velocity. Fluid momentum is continuously created, by either the downslope forces of gravity or a driving downstream pressure gradient (or a combination of the two), then transported toward the bottom boundary by molecular diffusion, and in the process is “consumed” by the resistance force at the bottom boundary.

**30** The tendency for molecular motions to even out the velocity distribution in a sheared fluid is in part the physical cause of the resistance of a fluid to shearing. In liquids the effect of transient molecular attractions in resisting shear is more important, but in gases the diffusive effect is the dominant one. The viscosity of a fluid is simply a measure of the effectiveness of molecular motions and/or molecular attractions in smoothing out an uneven velocity distribution or in maintaining the

velocity distribution against the tendency for the fluid to accelerate downslope and intensify the shearing. The continuum hypothesis allows us to disregard the details of molecular forces and diffusion and regard the resulting shear stress as a point quantity.

**31** *In turbulent flow*, on the other hand, there is an additional diffusional mechanism for transport of fluid momentum toward the boundary: exchange of macroscopic fluid eddies across the planes of mean shear parallel to the bottom tends to even out the velocity distribution by diffusion of momentum toward the bottom (Figure 4-11). By Newton's second law this rate of transport of momentum by turbulent motions is equivalent to a shear stress across the plane. This is called the **turbulent shear stress** or, usually, the **Reynolds stress**. It has exactly the same physical effect as an actual frictional force exerted directly between the two layers of fluid on either side of the plane: the faster-moving fluid above the plane exerts an accelerating force on the slower-moving fluid below the plane, and conversely the fluid below exerts an equal and opposite retarding force on the fluid above. It is true that the "range of operation" of this force is smeared out indefinitely for some distance on either side of the plane, but the result is the same as that of a force exerted directly across the plane.

**32** The total shear stress across a shear plane in the flow is the sum of the turbulent shear stress, caused by macroscopic diffusion of fluid momentum, and the viscous shear stress, caused in part by molecular diffusion of fluid momentum and in part by attractive forces between molecules at the shear plane. Owing to its macroscopic nature the turbulent shear stress can be associated with a given point on a shear plane only in a formal way; the viscous shear stress, although it has real physical meaning from point to point, must be regarded as an average over the area of the shear plane, because in turbulent flow both the magnitude and the orientation of shearing vary (continuously, and on the scale of eddies) from point to point.

---

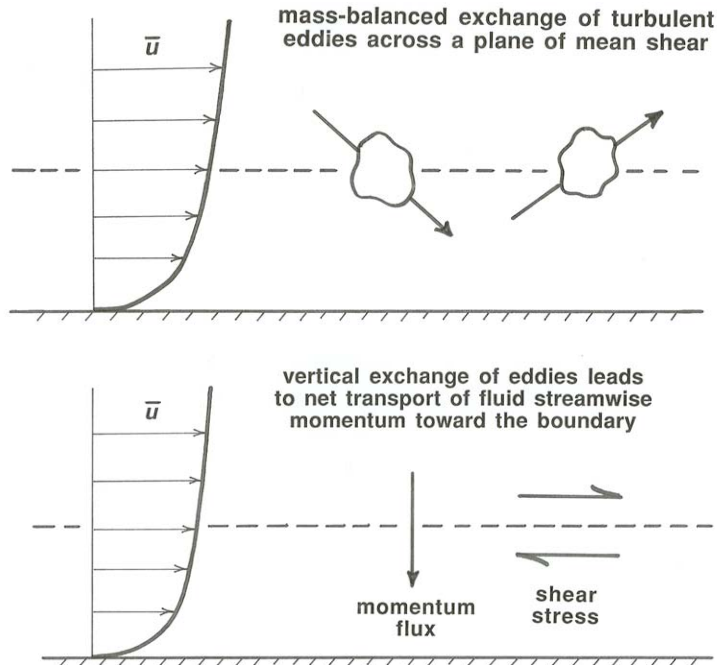


Figure 4-11. The origin of turbulent shear stress.

**33** In an earlier section of this chapter we derived expressions (Equation 4.3) for the shear stress across shear planes in laminar flow in a pipe or a channel. The shear stress in those two equations is the sum of the turbulent shear stress and the viscous shear stress. You may protest that the results in Equation 4.3 was obtained for laminar flow only. But in deriving the equations we did not assume anything at all about the internal nature of the flow, only that the flow is steady and uniform on the average. This is in contrast to the results for velocity distribution, Equation 4.7, which involve the assumption that the shear stress across a shear plane is given by Equation 1.8, an assumption that is inadmissible for turbulent flow because of the importance of the additional turbulent shear stress. The linear distribution of shear stress from zero at the surface to a maximum at the bottom should therefore hold just as well for turbulent flow as for laminar flow, provided only that the flow is steady and uniform on average.

**34** Except very near the solid boundary, where the normal-to-boundary component of the turbulent velocity must go to zero, the turbulent shear stress is far greater than the viscous shear stress. This is because turbulent exchange of fluid masses acts on a much larger scale than the molecular motions involved in the viscous shear stress and therefore transports momentum much more efficiently. Figure 4-12 is a plot of the

distribution of turbulent shear stress and viscous shear stress in steady uniform flow down a plane. The total shear stress is given by the straight line, and the turbulent shear stress is given by the curve that is almost coincident with the straight line all the way from the surface to very near the bottom but then breaks sharply away to become zero right at the bottom. The difference between the straight line for total shear stress and the curve for turbulent shear stress represents the viscous shear stress; this is important only very near the boundary.

**35** Because the turbulent shear stress is so much larger than the viscous shear stress except very near the boundary, differences in time-average velocity from layer to layer in turbulent flow are much more effectively ironed out over most of the flow depth than in laminar flow. This accounts for the much gentler velocity gradient  $du/dy$  over most of the flow depth in turbulent flow than in laminar flow; go back and look at Figure 4-8. But as a consequence of this gentle velocity gradient over most of the flow depth, near the bottom boundary, where viscous effects rather than turbulent effects are dominant, the velocity gradient is much steeper than in laminar flow, because the shearing necessitated by the transition from the still-large velocity *near* the boundary to the zero velocity *at* the boundary (remember the no-slip condition) is compressed into a thin layer immediately adjacent to the boundary.

### THE TURBULENCE CLOSURE PROBLEM

**36** When the Navier–Stokes equations are written for turbulent flow, and then instantaneous velocities are converted to their mean and fluctuating components, as was done in Chapter 3, time averages of products of fluctuating quantities (the Reynolds stresses mentioned in the previous section) emerge as new unknowns—and when one tries to characterize those new unknowns, further new unknowns arise! The result is that the equations of motion for turbulent flow can never form a closed system in which the number of equations is equal to the number of unknowns. This is called the *turbulence closure problem*. It is often said to be one of the great unsolved problems in all of physics. (That is a very strong statement.)

**37** Various strategies have been devised to circumvent the closure problem, by making certain assumptions or parameterizations. A simple and widely used example must suffice here: parameterizing the nature of turbulent momentum transport in a turbulent shear flow by use of the eddy viscosity, and how it varies from the boundary of the flow into the interior.

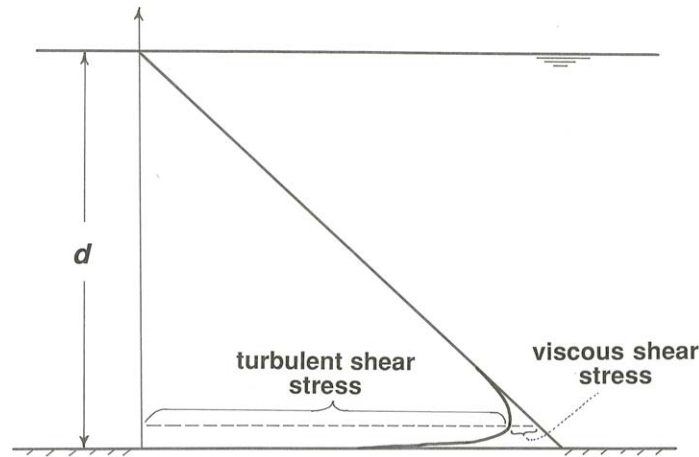


Figure 4-12. Distribution of total shear stress, turbulent shear stress, and viscous shear stress in a steady and uniform open-channel flow.

## STRUCTURE OF TURBULENT BOUNDARY LAYERS

### *Introduction*

**38** I have said quite a lot about what turbulence looks like in a general way, but now I need to be more specific about the structure of turbulence in turbulent boundary layers. (Another term I could use instead of turbulent boundary layers is *turbulent shear flow*: any turbulent flow that involves overall mean shearing, of the fluid, usually on account of the presence of a solid boundary to the flow.)

**39** Many of the important things about turbulence in boundary layers have been known for a long time. Workable techniques for reliable measurement of instantaneous velocities in air were developed half a century ago, in the 1940s and 1950s. Comparable laboratory techniques for water flows became available in the 1960s, and reliable field measurements in water flows became possible later. It is still difficult to make detailed observations of the scales, shapes, motions, and interactions of turbulent eddies, especially the relatively small eddies near the boundary. Only in the last few decades has observational knowledge of the dynamics of near-boundary turbulent structure advanced from the stage of point measurements of velocities and their statistical treatment, to observations of the eddy structure of the turbulent flow as a whole by means of various flow-visualization techniques. Studies on the structure and organization of turbulent fluid motions in boundary layers has become an actively growing

branch of fluid dynamics, and has resulted in much deeper understanding of the dynamics of turbulent flows.

**40** In the following section are some of the most important facts and observations on the turbulence structure of turbulent boundary layers—with steady uniform flow down a plane as a reference case, but the differences between this and other kinds of boundary-layer flow lie only in minor details and not in important effects.

### *Vertical Organization of Flow Structure in Channel Flows*

**41** First of all, you should expect the nature of turbulence to vary strongly from surface to bottom in the flow, because the boundary is the place where the vertical turbulent fluctuations must go to zero and where by the no-slip condition the fluid velocity itself must go to zero. You have already seen that the relative contributions of turbulent shear stress and viscous shear stress change drastically in the vicinity of the boundary.

**42** If the bottom boundary is physically smooth, or if it is rough but the height of the roughness elements is less than a certain value to be discussed presently, three qualitatively different but intergrading zones of flow can be recognized (Figure 4-13): a thin viscous sublayer next to the boundary, a turbulence-dominated outer layer occupying most of the flow depth, and a buffer layer between. If the boundary is too rough, the viscous sublayer is missing. Here I will only give a qualitative description of the flow in these layers; in later sections I will show their implications for flow resistance and velocity profiles.

**43** The *viscous sublayer* is a thin layer of flow next to the boundary in which viscous shear stress predominates over turbulent shear stress. Shear in the viscous sublayer, as characterized by the rate of change of average fluid velocity as one moves away from the wall, is very high, because fast-moving fluid is mixed right down to the top of the viscous sublayer by turbulent diffusion.

---

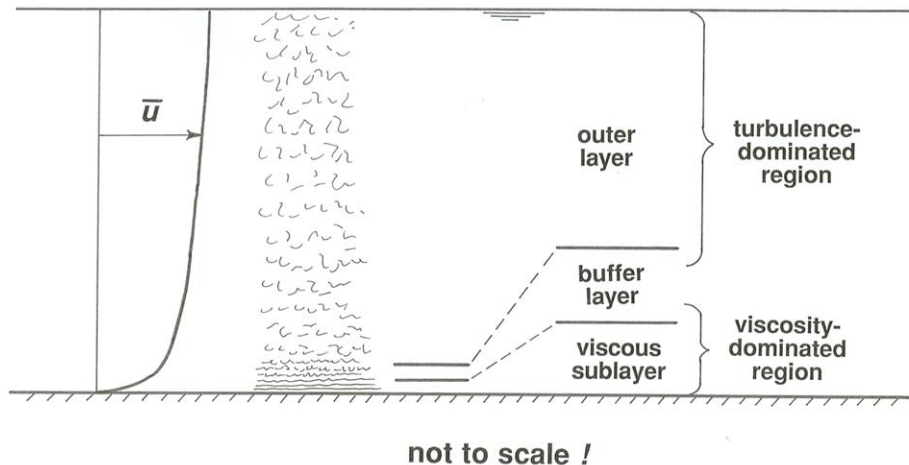


Figure 4-13. Division of turbulent open-channel flow into layers on the basis of turbulence structure.

**44** The thickness of the viscous sublayer depends on the characteristics of the particular flow and fluid; it is typically in the range of a fraction of a millimeter to many millimeters. You will find out later how to ascertain the viscous-sublayer thickness.

**45** The flow is not strictly laminar in the viscous sublayer because it experiences random fluctuations in velocity. What is important, however, is that because fluctuations in velocity normal to the boundary must decrease to zero at the boundary itself, molecular transport of fluid momentum is dominant over turbulent transport of momentum near the boundary. Fluctuations in velocity very close to the boundary must therefore be largely parallel to the boundary. Fluctuations in shear stress on the boundary itself caused by these fluctuations in velocity can be substantial. The turbulent fluctuations in velocity in the viscous sublayer are the result of advection of eddies from regions farther away from the wall; these eddies are damped out by viscous shear stresses in the sublayer.

**46** When the boundary is physically smooth the thickness of the viscous sublayer can easily be defined, but when the boundary is covered with closely spaced roughness elements (like sediment particles, or corrosion bumps, or densely spaced buildings, or trees and shrubs) with heights greater than the thickness of the viscous sublayer (or, more precisely, what the sublayer thickness would be in the absence of the roughness), then no sublayer is actually present at all, and turbulence extends all the way to the boundary, in among the roughness elements.

47 Of course, if you zoomed in to look at the boundary even more closely, you would find very thin viscous sublayers right at the surfaces of each of the roughness elements: close enough to any solid surface, the flow has to be dominated by viscous effects. In the preceding paragraph I was talking about the presence or absence of a viscous sublayer over a whole larger area of the boundary, at lateral scales much greater than the individual roughness elements.

48 The *buffer layer* is a zone just outside the viscous sublayer in which the gradient of time-average velocity is still very high but the flow is strongly turbulent. Its outstanding characteristic is that both viscous shear stress and turbulent shear stress are too important to be ignored. With reference to Figure 4-13 you can see that this is the case only in a thin zone close to the bottom. Very energetic small-scale turbulence is generated there by instability of the strongly sheared flow, and there is a sharp peak in the conversion of mean-flow kinetic energy to turbulent kinetic energy, and also in the dissipation of this turbulent energy; for this reason the buffer layer is often called the *turbulence-generation layer*. (There will be more on kinetic energy in turbulent flows soon.) Some of the turbulence produced here is carried outward into the broad outer layer of flow, and some is carried inward into the viscous sublayer. The buffer layer is fairly thin but thicker than the viscous sublayer.

49 The broad region outside the buffer layer and extending all the way to the free surface is called the *outer layer*. (In pipe flow this is more naturally called the *core region*.) This layer occupies most of the flow depth, from the free surface down to fairly near the boundary. Here the turbulent shear stress is predominant, and the viscous shear stress can be neglected. Except down near the buffer layer, turbulence in this zone is of much larger maximum scale than nearer the boundary. Because of their large size, the turbulent eddies here are more efficient at transporting momentum normal to the flow direction than are the much smaller eddies nearer the boundary; this is why the profile of mean velocity is much gentler in this region than nearer the bottom. But it turns out that these large eddies contain much less kinetic energy per unit volume of fluid than in the buffer layer. The normal-to-boundary dimension of the largest eddies in this outer layer is a large fraction of the flow depth—but there are smaller eddies too, at a whole range of scales; see a later section for more discussion of eddy scales.

50 In terms of the relative importance of turbulent shear stress and viscous shear stress, it is convenient to divide the flow in a somewhat different way (Figure 4-13) into a *viscosity-dominated region*, which includes the viscous sublayer and the lower part of the buffer layer, where

viscous shear stress is more important than turbulent shear stress, and a *turbulence-dominated region*, which includes the outer layer and the outer part of the buffer layer, where the reverse is true. In a thin zone in the middle part of the buffer layer the two kinds of shear stress are about equal. It is worth emphasizing that there are no sharp divisions in all this profusion of layers and regions: they grade smoothly one into another.

## FLOW RESISTANCE

### *Introduction*

**51** This section takes account of what is known about the mutual forces exerted between a turbulent flow and its solid boundary. You have already seen that flow of real fluid past a solid boundary exerts a force on that boundary, and the boundary must exert an equal and opposite force on the flowing fluid. It is thus immaterial whether you think in terms of resistance to flow or drag on the boundary.

### *Forces Exerted by a Flow on Its Boundary*

**52** What is the physical nature of the mutual force between the flow and the boundary? Remember that at every point on the solid boundary, no matter how intricate in detail the geometry of that boundary may be, two kinds of fluid forces act: *pressure*, acting normal to the local solid surface at the point, and *viscous shear stress*, acting tangential to the local solid surface at the point.

**53** If the boundary is physically smooth (Figure 4-14A) the downstream component of force the fluid exerts on the boundary can result only from the action of the viscous shear stresses, because the pressure forces can then have no component in the direction of flow. But the boundary may be strongly uneven or rough on a small scale at the same time it is planar or smoothly curving on a large scale; this unevenness or roughness might involve arrays of various kinds of bumps, corrugations, protuberances, or particulate masses. Most natural flows, and many in engineering practice also, like canals and corroded pipes, have physically rough boundaries. Then the picture is more complicated (Figure 4-14B), because there is a downstream component of pressure force on the boundary in addition to a downstream component of viscous force: just as with the drag on spheres, considered in Chapters 2 and 3, if roughness elements are present on the boundary, local pressure forces are greater on the upstream sides than on the downstream sides, so each element is subjected to a resultant pressure force with a component in the downstream direction.

---

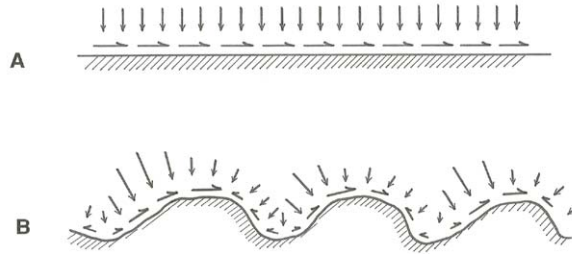


Figure 4-14. Pressure forces and viscous forces on physically smooth and physically rough boundaries.

---

**54** The details of pressure forces on roughness elements are complicated, because they depend not only on a Reynolds number based on the size of the roughness elements and the local velocity of flow around the elements (in generally the same way that the pressure forces depend on a Reynolds number in the case of unbounded and uniform flow around a sphere, as was discussed in earlier chapters), but also on the shape, arrangement, and spacing of the elements. Qualitatively, however, the picture is clear (Figure 4-15): at low Reynolds numbers the pressure force on an element is of the same order as the viscous force, as in creeping flow past a sphere, whereas at higher Reynolds numbers the pressure forces are much greater than the viscous forces, as in separated flow past a sphere.

**55** The sum of all the forces on individual roughness elements on the boundary (or, in the case of a physically smooth boundary, the sum of the viscous shear stresses at all points of the boundary) constitutes the overall drag on the boundary, or conversely the overall resistance to the flow; when expressed as force per unit area this boundary resistance is called the **boundary shear stress**, denoted by  $\tau_0$  (usually pronounced *tau-zero* or *tau-naught*). It is important to remember that  $\tau_0$  refers not to the viscous shear stress at any given point on the flow boundary—which seems to fit the description of “boundary shear stress” perfectly!—but to the average force per unit area, viscous forces plus pressure forces, over an area of the boundary large enough that the variations in local forces from point to point are suitably averaged out. That means an area many times the size of the individual roughness elements (Figure 4-16).

---

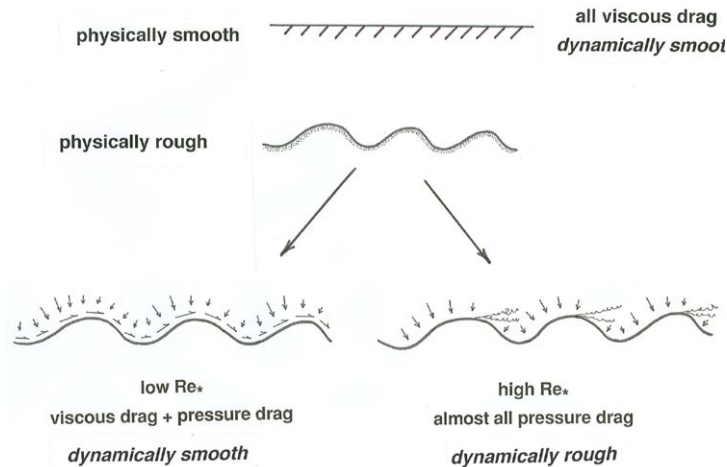


Figure 4-15. Differences in near-bed flow and forces in flow over a rough boundary, as a function of the roughness Reynolds number  $Re_*$ .

---

**56** It is worth considering at this point how the boundary shear stress  $\tau_0$  is actually measured in pipes and channels. Direct measurement is difficult even in the laboratory: mechanical shear plates set flush with the boundary tend to cause some disturbance to the flow because of the inevitable gap or step at the edges. Hot-film sensors, which measure the shear at the fluid–solid interface indirectly via the conductive heat transfer from a heated solid surface, get around this problem nicely for smooth boundaries, but they do not work well for rough boundaries, especially when the roughness elements are in motion, like sediment grains. Direct measurement under field conditions has been limited.

---

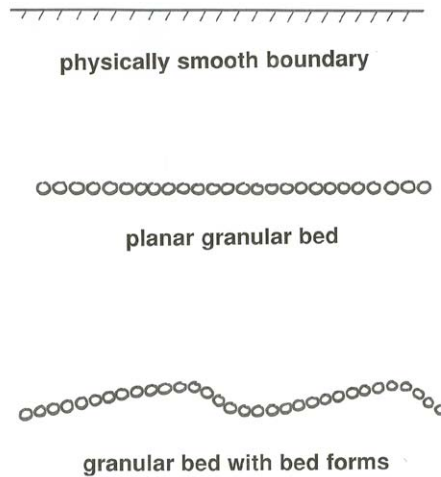


Figure 4-16. Boundary shear stress over physically smooth boundaries, granular-rough boundaries, and boundaries rough on the scale of bed forms as well as sediment particles.

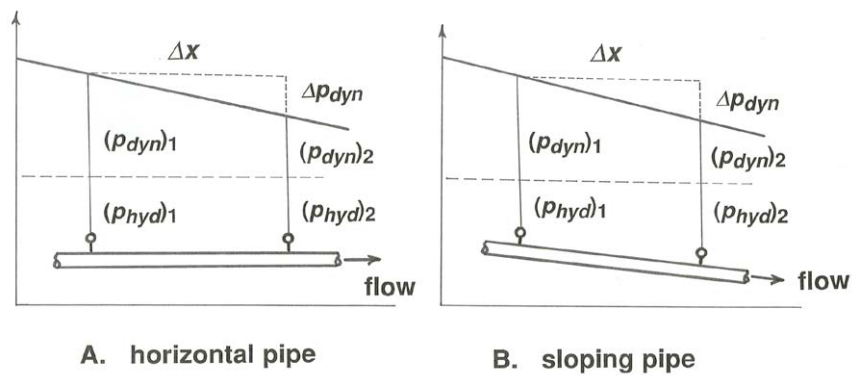


Figure 4-17. Static and dynamic pressure in **A)** a horizontal pipe and **B)** an inclined plane.

**57** Fortunately, there are other ways of measuring the boundary shear stress. In a horizontal closed conduit you can measure the downstream pressure gradient just by installing two pressure gauges some distance apart, reading the pressure drop, and dividing by the distance between the gauges (Figure 4-17A). Then you can use an equation, analogous to Equation 4.1, that relates the boundary shear stress to the pressure gradient. If the conduit is not horizontal, be sure to subtract out the difference in hydrostatic pressure between the two stations, so that you are left with the dynamic pressure (Figure 4-17B). In a steady and uniform channel flow you can use Equation 4.1, the resistance equation for channel flow, to find

$\tau_0$  without concern for the internal details of the flow simply by measuring the slope of the water surface; although not always a simple matter, this is possible in both field and laboratory with the proper surveying equipment. The problem is that the value of  $\tau_0$  obtained in this way is the average around the wetted perimeter of the cross section, so it is not exactly the same as the boundary shear stress at any particular place on the wetted perimeter. Moreover, if the channel flow is not uniform—if the depth and velocity vary from section to section—then Equation 4.1 holds only approximately, not exactly; the error introduced depends on the degree of nonuniformity.

**58** Another method of finding  $\tau_0$ , suitable only for laboratory experiments with smooth flow, is to measure the velocity profile within the viscosity-dominated zone of flow very near the boundary, using various techniques, in order to determine velocity gradient at the boundary, which by Equation 1.8 is proportional to  $\tau_0$ . One serious problem here is that the viscous sublayer is very thin, necessitating that the measuring device be extremely small for accurate results. Another problem is that this technique is not workable in situations where the roughness elements are larger than the potential thickness of the viscous sublayer—and that is true of most sediment-transporting flows of interest in natural environments.

**59** Finally, you will see presently, after considering velocity profiles in turbulent flow, that  $\tau_0$  can also be found indirectly in both rough and smooth flow by means of less demanding measurement of the velocity profile through part or all of the flow depth. This last method is the most useful of all.

### *Smooth Flow and Rough Flow*

**60** Two fundamentally different but intergrading cases of turbulent boundary-layer flow can be distinguished by comparing the thickness of the viscous sublayer and the height of granular roughness elements. (What I will say here is for sand-grain roughness, but the situation is about the same for close-packed roughness of any geometry.) The roughness elements may be small compared to the thickness of the sublayer and therefore completely enclosed within it (Figure 4-18A). Or they may be larger than what the sublayer thickness would be for the given flow if the boundary were physically smooth rather than rough (Figure 4-18B). In the latter case, flow over and among the roughness elements is turbulent, and the structure of this flow is dominated by effects of turbulent momentum transport. There can then be no overall viscous sublayer in the sense described in an earlier section, although, as noted earlier, a thin viscosity-dominated zone with thickness much smaller than the roughness size must

still be present at the very surfaces of all of the roughness elements. In the transitional case the roughness elements poke up through a viscous sublayer that is of about the same thickness as the size of the elements.

**61** If, in flow over a rough bed, the viscous-sublayer thickness is much greater than the size of the roughness elements, the overall resistance to flow turns out to be almost the same as if the boundary were physically smooth; such flows are said to be *dynamically smooth*



Figure 4-18. Differences in flow structure near a granular bed, depending upon whether **A)** the viscous sublayer is thicker than the heights of the particles or **B)** the heights of the particles are greater than what the thickness of the viscous sublayer would be in the absence of the particles.

(or hydraulically or hydrodynamically or aerodynamically smooth), even though they are in fact *geometrically* rough. (Obviously, flow over physically smooth boundaries is also dynamically smooth.) This is a consequence of the argument, introduced above, that if the Reynolds number of flow around individual roughness elements is small, as must be the case if the elements are much smaller than the viscous sublayer, pressure forces and viscous forces are of about the same magnitude, so that the presence of roughness makes little difference in the overall resistance to flow. If the elements are much larger than the potential thickness of the viscous sublayer, however, Reynolds numbers of local flow around the elements are large enough that pressure forces on the elements are much larger than viscous forces, and then the roughness has an important effect on flow resistance. Such flows are said to be *dynamically rough*. There is

an intermediate range of conditions for which the flow is said to be *transitionally rough*.

**62** It is convenient to have a dimensionless measure of distance from the boundary that can be used to specify the thicknesses of the viscous sublayer and the buffer layer. Assume for this purpose that the dynamics of flow near the boundary is controlled only by the shear stress  $\tau_0$  and the fluid properties  $\rho$  and  $\mu$ . This should seem at least vaguely reasonable to you, in that the dynamics of turbulence and shear stress in the viscous sublayer and buffer layer are a local phenomenon related to the presence of the boundary but not much affected by the weaker large-scale eddies in the outer layer. There will be more on this in the later section on velocity profiles. You can readily verify that the only possible dimensionless measure of distance  $y$  from the boundary would then be  $\rho^{1/2}\tau_0^{1/2}y/\mu$ , often denoted by  $y^+$ . A similar dimensionless variable  $\rho^{1/2}\tau_0^{1/2}D/\mu$ , involving the height  $D$  of roughness elements on the boundary, can be derived by the same line of reasoning about variables important near the boundary. This latter variable is called the *boundary Reynolds number* or the *roughness Reynolds number*, often denoted by  $Re_*$ .

**63** The dimensionless distance  $y^+$  and the roughness Reynolds number  $Re_*$  can be written in a more convenient and customary form by introduction of two new variables. The quantity  $(\tau_0/\rho)^{1/2}$ , usually denoted by  $u_*$  (pronounced *u-star*), has the dimensions of a velocity; it is called the *shear velocity* or the *friction velocity*. Warning:  $u_*$  is *not* an actual velocity; it is a quantity involving the boundary shear stress that conveniently has the dimensions of a velocity. The quantity  $\mu/\rho$ , which you may have noticed commonly appears in Reynolds numbers, is called the *kinematic viscosity*, denoted by  $\nu$ . The word *kinematic* is used because the dimensions of  $\nu$  involve only length and time, not mass. If  $y^+$  as defined above is rearranged slightly it can be written  $u_*y/\nu$  and the roughness Reynolds number can be written  $u_*D/\nu$ .

**64** When expressed in the dimensionless form  $y^+$ , the transition from the viscous sublayer to the buffer layer is at a  $y^+$  value of about 5, and the transition from the buffer layer to the turbulence-dominated layer is at a  $y^+$  value of about 30. These transition values are about the same whatever the values of boundary shear stress  $\tau_0$  and fluid properties  $\rho$  and  $\mu$ ; this confirms the supposition made above that over a wide range of turbulent boundary-layer flows the variables  $\tau_0$ ,  $\rho$ , and  $\mu$  suffice to characterize the flow near the boundary. These values are known not from watching the flow but from plots of velocity profiles, as will be discussed presently.

**65** The relative magnitude of the viscous-sublayer thickness and the roughness height  $D$  can be expressed in terms of the roughness Reynolds

number  $u_* D/\nu$ . To see this, take the top of the viscous sublayer to be at  $u_* \delta_v/\nu \approx 5$ , meaning that  $\delta_v \approx 5\nu/u_*$  is the distance from the boundary to the top of the viscous sublayer. Here I have replaced  $y$  by  $\delta_v$ , the thickness of the viscous sublayer. The ratio of particle size to sublayer thickness is then  $D/\delta_v \approx (u_* D/\nu)/5$ . In other words, sublayer thickness and particle size are about the same when the roughness Reynolds number has a value of about 5. (But remember that if the roughness elements are this large or larger, there is no well developed viscous sublayer in the first place.) Another way of looking at this is that we can compare the particle size  $D$  with  $\nu/u_*$ , a quantity with dimensions of length called the *viscous length scale*, which is proportional to the thickness of the viscous sublayer.

**66** The limits of smooth and rough flow can also be specified by values of the roughness Reynolds number. The upper limit of smooth flow is associated with the condition that the height of the viscous sublayer is about equal to that of the roughness elements. As noted above, at the top of the viscous sublayer  $y^+ = u_* \delta_v/\nu \approx 5$ , so the upper limit of roughness Reynolds numbers for smooth flow should be  $u_* D/\nu \approx 5$ , and in fact the value of 5 is in good agreement with results based on both boundary resistance and velocity profiles. Likewise, the lower limit of roughness Reynolds numbers for fully rough flows is found to be about 60. It is between these values ( $5 < u_* D/\nu < 60$ ) that the flow is said to be transitionally rough.

**67** Some further discussion of smooth and rough flow can be found in the latter part of this chapter in the section on velocity profiles.

### *Dimensional Analysis of Flow Resistance*

**68** One circumstance that tends to make the standard treatments of flow resistance in fluid-dynamics textbooks seem more complicated than they really are is that the details of the equations for flow resistance (although not their general form) depend not only on the boundary roughness but also on the overall geometry of the flow. On the one hand, the flow may be a turbulent boundary layer growing into a free stream; on the other hand, it may be a fully established turbulent boundary layer that occupies all of a conduit or channel. In terms of flow mechanics in the boundary layer itself, these two kinds of flow can be treated together. In the latter case any number of boundary geometries are possible. The classic experiments on flow resistance were made using circular pipes with inside surfaces coated with uniform sand, and not much systematic work has been done on channel flow. The discussion here focuses on pipe flow, with the understanding that both the principles and the general form of the results are the same for any steady uniform flow whatever the boundary geometry.

**69** In common with other aspects of turbulent boundary-layer flow, there is no theory we can draw on to find relationships for flow resistance. It is therefore again natural to start with a dimensional analysis of resistance to flow through a circular pipe or tube (Figure 4-19) in order to develop a framework in which experimental data can provide dimensionless relationships that are expressible in the form of essentially empirical equations that are valid in certain ranges of flow.

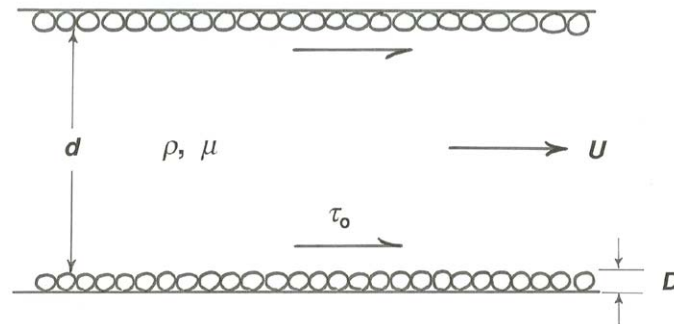


Figure 4-19. Definition sketch for dimensional analysis of flow resistance in a circular pipe.

---

**70** Which variables must be specified in order that the boundary shear stress  $\tau_0$  can be fully characterized or determined? Pipe diameter  $d$  and mean flow velocity  $U$  are important because they affect the rate of shearing in the flow, both directly and through their effect on the structure of turbulence. Viscosity  $\mu$  is obviously important because of its role in determining viscous shear stress at the boundary. Fluid density  $\rho$  is important because if the flow is turbulent there must be local fluid accelerations. Finally, the size  $D$  of boundary roughness elements may affect the turbulent forces and motions near the boundary. There are thus two important length scales in the problem of flow resistance: pipe diameter and roughness height. We will have to assume that shape, spacing, and arrangement of the roughness elements are either always the same or, if variable, are of secondary importance in determining flow resistance. Neither assumption is justified, but they form a good place to start. Never mind that if the boundary is rough there is some haziness about where the position of the wall should be taken in defining the pipe diameter; at least with respect to flow resistance, any reasonable choice

produces consistent results provided that consideration is limited to geometrically similar roughness.

**71** Assuming that all of the important variables have been included,  $\tau_o$  can be viewed as a function of the five variables  $U$ ,  $d$ ,  $D$ ,  $\rho$ , and  $\mu$ . You should then expect to have a dependent dimensionless variable as a function of two independent dimensionless variables. It should occur to you immediately that one of the independent dimensionless variables can be a Reynolds number based on  $U$  and  $d$ , which I will call the mean-flow Reynolds number. The other independent dimensionless variable is most naturally  $d/D$ , the ratio of pipe diameter to roughness height. This variable is called the **relative roughness**. The dependent dimensionless variable, which must involve  $\tau_o$ , has exactly the same form and physical significance as the dimensionless drag force or drag coefficient that characterizes the drag on a sphere moving relative to a fluid (Chapter 2), except that here we are dealing with a force per unit area rather than with a force. You can verify that one possible dimensionless variable involving  $\tau_o$  is  $8\tau_o/\rho U^2$ , and although this is not the only one possible (there are two others; you might at this point try to find them yourself) it is the most useful, and it is the one that is conventionally used. (The factor 8 is present for reasons of convenience that need not concern us here.) This dimensionless boundary shear stress is called the **friction factor**, denoted by  $f$ ; it is one kind of flow-resistance coefficient.

**72** The functional relationship for flow resistance can thus be written

$$f = \frac{8\tau_o}{\rho U^2} = F\left(\frac{\rho U d}{\mu}, \frac{d}{D}\right) \quad (4.8)$$

where  $F$  is a function that for turbulent flow has to be ascertained by experiment.

### **Resistance Diagrams**

**73** The relationship expressed in Equation 4.8 can be shown in a two-dimensional graph most easily by plotting curves of  $f$  vs. Reynolds number for a series of values of  $d/D$ . Figure 4-20 shows a graph of this kind, called a **resistance diagram**. The data were obtained by Nikuradse (1933) for flows through circular pipes lined with closely spaced sand grains of approximately uniform size. A version of Figure 4-20 is shown in just about all books on flow of viscous fluids.

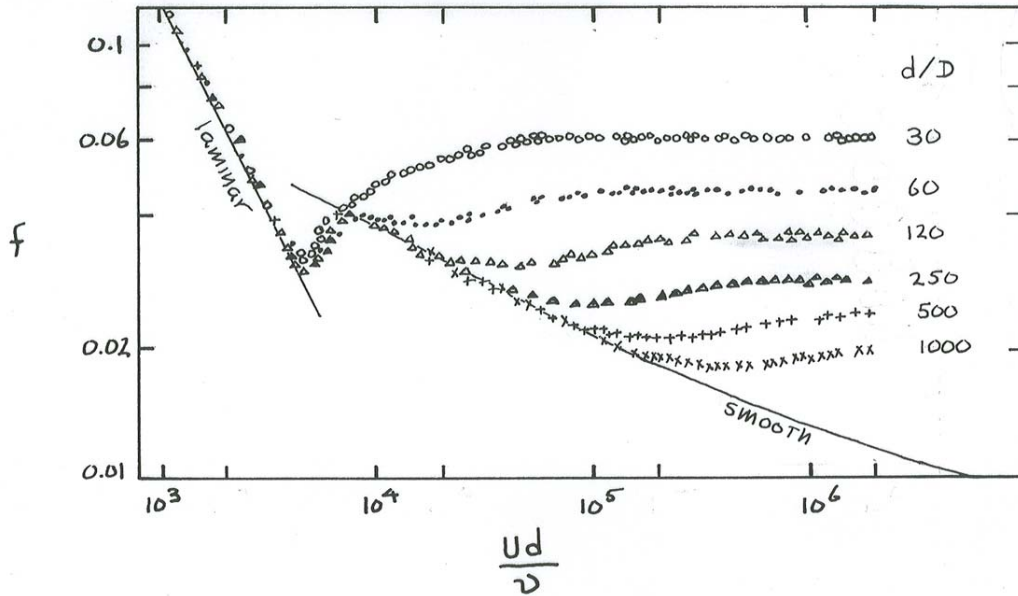


Figure 4-20. Graph of friction factor vs. mean-flow Reynolds number (pipe friction diagram) for a flow in a circular pipe with granular roughness.

74 Leaving aside the steeply sloping part of the curve on the far left (it holds for laminar flow in the pipe, for which we have already obtained an exact solution), you see that at fairly low Reynolds numbers the curve of  $f$  vs.  $Re$  for any given  $d/D$  in Figure 4-20 at first slopes gently down to the right, then breaks away, and finally levels out to a horizontal straight line. The larger the relative roughness  $d/D$  the greater the Reynolds number at which the breakaway takes place. Physically smooth boundaries, for which  $D/d = 0$ , follow the descending curve to indefinitely high Reynolds numbers. Flows that plot on this descending curve are those I earlier termed *dynamically smooth*. Note that flows over physically rough boundaries can be dynamically smooth, provided that  $d/D$  is sufficiently large. If  $Re$  is fairly small and the pipe is fairly large,  $D$  can be absolutely large—millimeters or even centimeters—in smooth water flows. Flows that plot on the horizontal straight lines to the right are those I called fully rough, and those at intermediate points are those I called transitionally rough. For a given  $d/D$  the flow is smooth at low Reynolds numbers but rough at sufficiently high Reynolds numbers.

75 Two questions need to be discussed at this point:

- How would the results in Figure 4-20 change for kinds of roughness elements different from glued-down uniform sand grains?
- How would the results change for conduits or channels with geometry different from that of a circular pipe?

The answer to both of these questions is that the results are qualitatively the same, provided that the characteristics of the roughness are not grossly different and that the size of the roughness elements remains a small fraction of the conduit diameter or channel depth. The curves are merely shifted slightly in position or differ slightly in shape. To adapt the uniform-sand-roughness results to other kinds of roughness a quantity called the *equivalent sand roughness*, denoted by  $k_s$ , is defined as the fictitious roughness height that would make the results for the given kind of roughness expressible by the same plot as in Figure 4-20 for uniform-sand-roughness pipes. And to compare the pipe results with those for conduits or channels with different geometry, it is customary to use the hydraulic radius in place of the pipe radius, although the results cannot be expected to be exactly the same. By applying the definition of hydraulic radius given earlier in this chapter you can verify that for a circular pipe the hydraulic radius specializes to one-fourth the pipe diameter. (You have already seen that for an infinitely wide channel flow the hydraulic radius specializes to the flow depth.)

**76** There is an equivalent way of expressing resistance that is used specifically for open-channel flow. Combining the equation  $\tau_0 = (f/8)\rho U^2$  that defines the friction factor  $f$  with the equation  $\tau_0 = \rho g d \sin \alpha$  (Equation 4.1) for boundary shear stress in steady uniform flow down a plane, eliminating  $\tau_0$  from the two equations, and then solving for  $U$ ,

$$U = \left( \frac{8g}{f} d \sin \alpha \right)^{1/2} \quad (4.9)$$

$$U = C(d \sin \alpha)^{1/2} \quad (4.10)$$

where

$$C = \left( \frac{8g}{f} \right)^{1/2} \quad (4.11)$$

77 Equation 4.11, which relates mean velocity, flow depth, and slope for uniform flow in wide channels, is called the *Chézy equation*, after the eighteenth-century French hydraulic engineer who first developed it. The coefficient  $C$ , called the *Chézy coefficient*, is *not* a dimensionless number like the friction factor  $f$ ; it has the dimensions  $g^{1/2}$ . But because  $g$  is very nearly a constant at the Earth's surface,  $C$  can be viewed as being a function only of  $f$ . I have introduced the Chézy  $C$  because it is in common use in work on open-channel flow, but you should understand that it adds nothing new.

## VELOCITY PROFILES

### *Introduction*

78 You have already seen that the profile of time-average local fluid velocity  $\bar{u}$  from the bottom to the surface in turbulent flow down a plane is much blunter over most of the flow depth than the corresponding parabolic profile for laminar flow (Figure 4-8). This is the place to amplify and quantify the treatment of velocity profiles in turbulent boundary-layer flows.

79 First I will pose the following question: Can an equation for the velocity profile in a turbulent boundary-layer flow be found by writing an equation like Equation 1.8 for turbulent flow and solving for the velocity profile by integration? As noted earlier, Equation 4.4, for the distribution of total shear stress in the flow, is valid for turbulent flow as well as for laminar flow, because no assumptions were made about the nature of internal fluid motions in its derivation, just that the flow must be steady and uniform on the average. And an expression of the same kind as Equation 1.8, defining the shear stress, can also be written for turbulent flow:

$$\tau = \mu \frac{du}{dy} + \eta \frac{du}{dy} \quad (4.12)$$

80 The term  $\mu(du/dy)$  is the *viscous shear stress* due to the mean shear across planes parallel to the boundary. (Actually it's is a spatial average over an area of such a plane that is large relative to eddy scales, because fluid shear varies from point to point in turbulent flow.) The term  $\eta(du/dy)$  is a way of writing the *turbulent shear stress* across these planes that involves an artificial quantity  $\eta$ , called the *eddy viscosity*, that is formally like the molecular viscosity  $\mu$ . Everywhere in a turbulent shear flow except very near the solid boundary the eddy viscosity is much larger than the molecular viscosity, because turbulent momentum transport is dominant

over molecular momentum transport. (Often  $\eta$  is written as  $\rho\varepsilon$ , where  $\varepsilon$  can be viewed as the *kinematic eddy viscosity*, in analogy with  $\nu$ ;  $\varepsilon$  is also called the *eddy diffusion coefficient*.) Just as for laminar flow, the expressions for  $\tau_0$  in Equation 4.12 and Equation 1.8 can be set equal to give a differential equation for  $u$  as a function of distance  $y$  from the boundary:

$$(\mu + \eta) \frac{du}{dy} = \gamma \sin \alpha (d - y) \quad (4.13)$$

**81** Unfortunately there is always an insuperable problem in integrating Equation 4.13, or any other equation like it for turbulent flow in a conduit or channel with some other geometry, to find the velocity distribution. Unlike the molecular viscosity  $\mu$ , the eddy viscosity  $\eta$ , rather than being a property of the fluid, depends upon the flow: it varies with height above the boundary, because the turbulent shear stress it represents is a function of the flow itself, for which we are trying to solve. We are therefore always forced to find the velocity distribution in turbulent flow by experiment.

**82** It is important to realize, however, that experiments to find the velocity profile do not have to be blindly empirical: physical reasoning can be used to guess which effects and therefore which variables are important in governing the velocity distribution in the various layers of the flow. If the functional relationships thus specified by the dimensional structure of the problem are consistent with the observational results, then the correctness of that qualitative view of the physics is confirmed. In fact, much of what is known about turbulent flow past solid boundaries has been learned in this way.

**83** We will stick with steady and uniform flow down a plane, but exactly the same kind of analysis could be made for flow in a closed conduit. Think about which variables you have to specify to take full account of the profile of time-average velocity  $u$  along an imaginary line through the flow, normal to the bottom boundary, stretching from the bottom to the free surface (Figure 4-21).

---

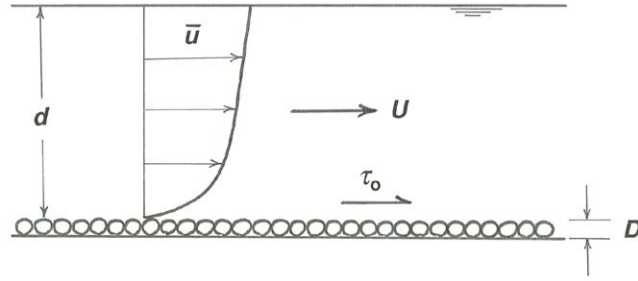


Figure 4-21. Definition sketch for dimensional analysis of velocity profiles in turbulent open-channel flow.

**84** The bottom can be either smooth or rough. As in the flow-resistance problem, make the assumption (not a good one, but it gets us started) that the roughness can be characterized by the size  $D$  of the elements without having to worry about their shape and arrangement. The boundary shear stress  $\tau_0$  is the best variable to use to characterize the strength of the flow. You should expect that in general the flow depth  $d$  would be needed as well. The viscosity  $\mu$  is needed, because it is tied up with shearing in the fluid. Finally, as in all problems in turbulent flow, the fluid density  $\rho$  is needed, because the fluid experiences local accelerations (in the form of eddies), so fluid inertia is important. So  $\bar{u}$  can be viewed as a function of  $\tau_0$ ,  $\rho$ ,  $\mu$ ,  $d$ , and  $D$ , and of course the distance  $y$  above the bottom:

$$\bar{u} = f(\tau_0, \rho, \mu, D, d, y) \quad (4.14)$$

The dimensionless functional relationship for  $\bar{u}$  is then

$$\frac{\bar{u}}{u_*} = f\left(\frac{u_* D}{\nu}, \frac{d}{D}, \frac{y}{d}\right) \quad (4.15)$$

where we have made use of the shear velocity  $u_*$  and the kinematic viscosity  $\nu$  introduced earlier in this chapter. Equation 4.15 says that  $\bar{u}/u_*$ , a dimensionless version of  $\bar{u}$  (often denoted  $u^+$ ), should be a function only of the roughness Reynolds number  $u_* D/\nu$  and the relative roughness  $d/D$  for a given dimensionless position  $y/d$  in the flow. There are alternative possibilities for the three independent dimensionless variables (for example, all three could be put into the form of a Reynolds number, each

with a different one of the three length variables), but this is the most natural.

**85** I am sure that all the velocity data you could get your hands on would plot very nicely in a four-dimensional graph using the variables  $\bar{u}/u_*$ ,  $u_*D/\nu$ ,  $d/D$ , and  $y/d$ . But even though the number of variables has been reduced from seven to four, you would still have a burdensome plotting job and a product that would be unwieldy for practical use. Moreover, further careful study would be needed to decipher what the graph is telling you about the physics behind velocity profiles. This is a good place to think about whether the problem can be simplified further by a divide-and-conquer approach wherein certain of the variables are eliminated or modified in certain ranges of conditions to arrive at simpler functions that represent the data well under those conditions. This serves two purposes: it provides useful results, and it helps to clarify the physical effects that are important.

**86** First off, in the next two sections, I will present some ideas about *energy in turbulent flow*. This may seem out of place here, but it leads to two conclusions that are of great importance for velocity profiles in turbulent flow: that of

- the existence of overlapping inner and outer layers of the flow, in which separate equations for velocity profiles hold, and that of
- the approximate independence of these profiles on the mean-flow Reynolds number.

Further subsections are devoted to the details of velocity profiles in the inner and outer layers of flows for which the diameter of the sediment on the bed is far smaller than the flow depth.

### *Energy*

**87** In making some simplifying assumptions it helps to take a closer look at the nature of turbulence in a channel flow. I will present some arguments that I hope will make some sense to you even though they cannot be developed rigorously here. In what follows, remember that kinetic energy, a quantity  $mv^2/2$  associated with a body with mass  $m$  moving with velocity  $v$ , is changed only when an unbalanced force does work on the body, and the change in kinetic energy is equal to the work done. The change in kinetic energy caused by the action of certain forces like gravity can be recaptured without any loss of mechanical energy, but

the work done by frictional forces represents conversion of mechanical energy into heat.

**88** I will start with laminar flow because the energy bookkeeping is simpler (Figure 4-22A). The viscous shear stress acting across the shear planes does work against the moving fluid. (Remember that a force does work on a moving body provided that there is a component of the force in the direction of movement of the body, as is the case here.) The viscous shear stress is the

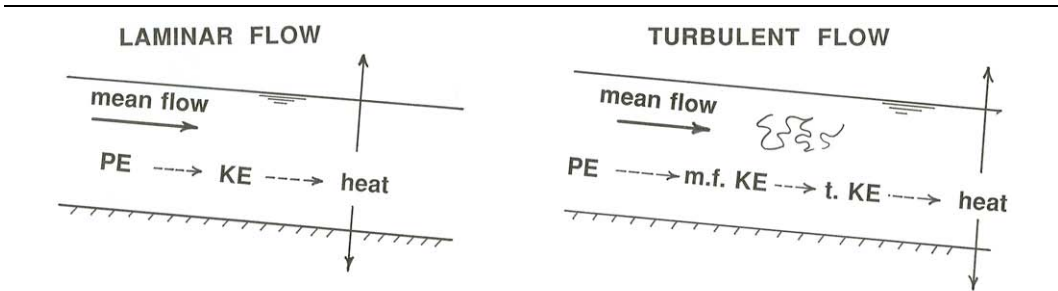


Figure 4-22. Energetics of **A)** laminar open-channel flow and **B)** turbulent open-channel flow.

mechanism that converts potential energy into heat, the heat then being transferred to the surroundings by conduction or radiation. The particular magnitude of kinetic energy in the flow in the process of this conversion is an outcome of the dynamics of the flow.

**89** In turbulent flow (Figure 4-22B), kinetic energy is contained not just in the mean flow but also in the turbulent fluctuations. Potential energy is again converted to heat, but the way the flow mediates this conversion, and therefore the picture of kinetic energy in the flow, is more complicated. This is because energy is extracted mainly by the work done against the mean motion by the turbulent shear stress rather than by the viscous stress, because at all levels in the flow except very near the bottom the former greatly overshadows the latter. This work done by the turbulent shear stress transforms the kinetic energy of the mean motion into kinetic energy associated mostly with the largest eddies, which have the dominant role in the turbulent shear stress because they are the longest-range carriers of fluid momentum. But not much of this turbulent kinetic energy is converted directly into heat in these large eddies, because they are so large relative to the velocity differences across them that shear rates in them are very small.

**90** Then where does the kinetic energy go? Answer: it is handed down to smaller eddies. This phrase “handed down” might strike you as plausible but unilluminating. Large eddies degenerate or become distorted into smaller eddies in ways not elaborated here, and when this happens the kinetic energy that was associated with the large eddies becomes “transferred to” (that is, is now associated with) the smaller eddies. But the odds are all against smaller eddies organizing themselves again into larger eddies—just watch the breakup of regular flow in a smoke plume to get the sense that the natural tendency in turbulent motions is for larger-scale motions to be broken up into smaller-scale motions. So in terms of kinetic energy, turbulence is largely a one-way street: it passes energy mostly from large scales to small scales, not in the other direction. This effect is called an *energy cascade*. Shear rates are greatest in the smallest eddies because of their small size relative to the velocity differences across them, and it is in these smallest eddies that most of the kinetic energy is finally converted into heat. In fact, the reason why there is a lower limit to eddy size is that below a certain scale the viscous shear stresses are so strong that they damp out the velocity fluctuations.

**91** A very significant consequence is that viscosity has a direct effect on turbulence only at the smallest scales of turbulent motion. If the mean-flow Reynolds number is increased, the energy cascade is lengthened at the smallest scales by development of even smaller eddies, but the structure of turbulence at larger scales is not much changed (Figure 4-23). So any bulk characteristic of the flow that is governed by the large-scale turbulence—like the velocity profile, which depends mainly on the turbulent exchange of fluid momentum—should be only slightly dependent on the Reynolds number. This effect is called *Reynolds-number similarity*.



Figure 4-23. Increase in the range of eddy scales as a function of mean-flow Reynolds number.

---

### *Inner and Outer Layers*

**92** Now back to velocity profiles. I want to convince you that two different but overlapping regions or layers of the flow can be recognized (Figure 4-24) in which the velocity profile depends not on the full list of variables  $\tau_0$ ,  $\rho$ ,  $\mu$ ,  $D$ ,  $y$ , and  $d$  used in the dimensional

analysis above but on certain subsets. The advantage is that in each of these layers there is then a simpler functional relationship for the velocity profile, one that leads to a curve in a two-dimensional graph that holds very well for almost the entire range of turbulent channel flows. I will wave my arms a little about the various variables, but of course the most convincing evidence is that this is how things actually work out, as you will see.

**93** Near the bottom boundary, in what I called the buffer zone and for a ways outside it, the turbulence is small-scale and intense, and both production and dissipation of turbulent kinetic energy are known from actual measurements to be at a peak. It is reasonable to view the dynamics of the turbulence, and therefore the nature of the velocity profile, as being controlled by local effects and substantially independent of the nature of the turbulence in the rest of the flow, all the way up to the free surface. This is also true of the viscous sublayer, if one is present, because there the velocity profile is controlled by the strong viscous shear adjacent to the solid boundary. The velocity profile in this inner layer thus depends on  $\tau_0$ ,  $D$ ,  $\rho$ ,  $\mu$ , and  $y$ , but not on  $d$ .

---

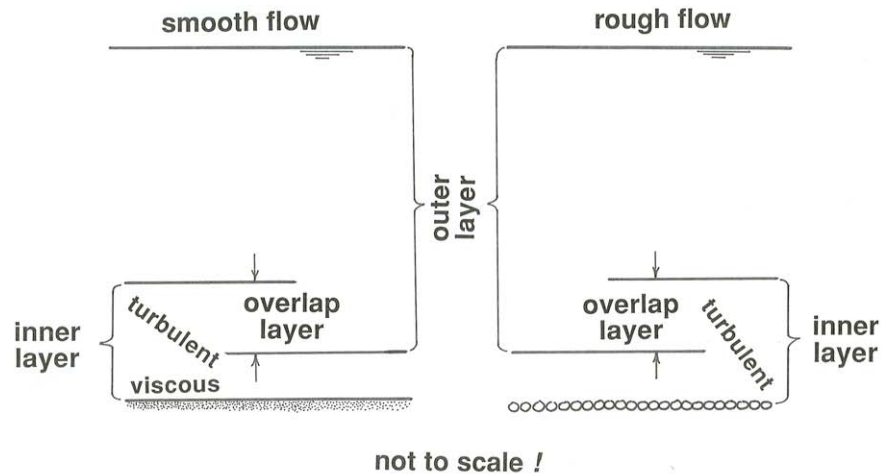


Figure 4-24. Layers in turbulent open-channel flow.

**94** On the other hand, over most of the flow depth, from the free surface all the way down to the top of the buffer layer in smooth flow, you have seen already from the discussion of turbulent energy that the velocity profile should be largely independent of  $\mu$ . If the boundary is rough, the profile should be independent of  $D$  as well as of  $\mu$  down to a position just far enough above the roughness elements that the turbulence shed by the elements is not important in the turbulence dynamics. But you should expect the profile to depend on  $d$ , because the size of the largest eddies is proportional to the flow depth. The velocity profile in this outer layer (here I have generalized the significance of the concept of the outer layer introduced in an earlier section) should thus depend on  $\tau_0$ ,  $\rho$ ,  $d$ , and  $y$ , but not on  $D$  or  $\mu$ .

**95** If you scrutinize the definitions of the inner and outer layers in the last two paragraphs in the light of what I have said about the structure of the flow, you will see that *they are likely to overlap*. In other words, there is a zone where the velocity profile is at the same time independent of all three variables  $d$ ,  $\mu$ , and  $D$ . This should be true so long as the mean-flow Reynolds number is high enough (well beyond the laminar–turbulent transition) that the viscosity-dominated zone near the boundary is very thin relative to the flow depth. (Remember that the thickness of the viscous sublayer decreases as the Reynolds number increases, because the Reynolds number is a measure of the relative importance of inertial forces and viscous forces.)

**96** You are probably thinking by now that I have presented you with a confusion of layers. I will summarize them at this point. On the one hand, in terms of the relative importance of viscous shear stress and turbulent shear stress it is natural to recognize three intergrading but well defined zones (the viscous sublayer, the buffer layer, and the outer layer) or, more generally, a viscosity-dominated layer below and a turbulence-dominated layer above. On the other hand, in terms of importance or unimportance of variables (a related but not identical matter), two overlapping layers can be recognized: an inner layer in which the mean velocity, and other mean characteristics of the flow as well, depends on  $\mu$  or  $D$  (or both) but not  $d$ , and the same outer layer in which the mean velocity depends on  $d$  but not on  $\mu$  or  $D$ . In rough flow the entire thickness of the flow is dominated by turbulence, and there is no viscosity-dominated layer—but there are still inner and outer layers.

### *The Law of the Wall for Smooth Boundaries*

**97** Look first at the inner-layer velocity profile over a physically smooth bottom boundary. From what was just said about the inner layer,

$$\bar{u} = f(\tau_0, \rho, \mu, y) \quad (4.16)$$

or in dimensionless form,

$$\frac{\bar{u}}{u_*} = f\left(\frac{\rho u_* y}{\mu}\right) \quad (4.17)$$

Equation 4.17 states that the velocity  $\bar{u}$ , nondimensionalized using  $u_*$ , depends only on  $y^+$ , the dimensionless distance from the bottom. So the velocity profile should be expressible as a single curve for all turbulent channel flows with smooth bottom boundaries. Equation 4.17 is the general form of what is called *the law of the wall for smooth boundaries*.

**98** You should expect the velocity profile expressed in Equation 4.17 to be in two parts, one corresponding to the viscous sublayer and the other to the outer part of the inner layer, where turbulent shear stress predominates over viscous shear stress. These two parts of the profile have to pass smoothly one from the other in the intervening buffer layer. Because fluid accelerations are unimportant in the viscous sublayer,  $u$  there depends on  $\tau_0$ ,  $\mu$ , and  $y$ , but not on  $\rho$ .

$$\bar{u} = f(\tau_0, \mu, y) \quad (4.18)$$

The only way to write Equation 4.28 in dimensionless form is

$$\frac{\mu u}{\tau_0 y} = \text{const} \quad (4.19)$$

because there is only one way to form a dimensionless variable from the four variables  $\bar{u}$ ,  $\tau_0$ ,  $\mu$ , and  $y$ . Equation 4.19 can be juggled algebraically a little by introducing  $\rho$  on both sides, for no other reason than to put it in the same form as Equation 4.17:

$$\frac{\bar{u}}{u_*} = \text{const} \frac{\rho u_* y}{\mu} \quad (4.20)$$

**99** The constant in Equation 4.20 turns out to be unity. To get an idea why, go back to Equation 4.7, the exact solution for the velocity profile in laminar channel flow. It is reasonable to expect that the velocity profile in the viscous sublayer of a turbulent channel flow is like the velocity profile near the boundary in a laminar channel flow. Points near the boundary in laminar flow, where the velocity gradient  $d\bar{u}/dy$  is very large, are way out on the limb of the parabola in Equation 4.7, so the second term on the right in Equation 4.7 can be neglected and  $\bar{u}$  assumed to be a linear function of  $y/d$ :

$$\bar{u} = \frac{\tau_0}{\mu d} (y d) \quad (4.21)$$

When cast in the same form as Equation 4.30, this becomes

$$\frac{\bar{u}}{u_*} = \frac{\rho u_* y}{\mu} \quad (4.22)$$

Equation 4.22 represents the specific part of the law of the wall for a dynamically smooth flow inside the viscous sublayer. Figure 4-25 shows that Equation 4.22 is in good agreement with careful velocity measurements in the viscous sublayer.

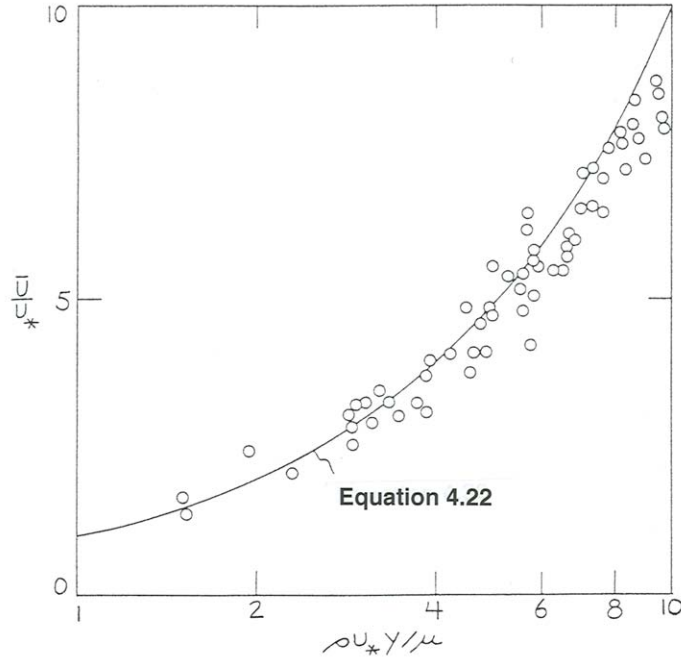


Figure 4-25. Plot of dimensionless mean flow velocity  $\bar{u}/u_*$  vs. dimensionless distance from boundary,  $\rho u_* y/\mu$ , for the viscous sublayer in turbulent open-channel flow. This plot represents the law of the wall inside the viscous sublayer.

**100** In the outer, turbulence-dominated part of the inner layer over a physically smooth bottom, we can assume that  $d\bar{u}/dy$  does not depend on  $\mu$ , because the shear stress and therefore the velocity gradient is determined almost entirely by turbulent momentum exchange (see Equation 4.12). On the other hand,  $\bar{u}$  itself must depend on  $\mu$ , because the velocity profile in the turbulence-dominated part of the inner layer must be connected to that in the viscosity-dominated part, and you have just seen that the velocity profile in the viscous sublayer depends on  $\mu$ . In other words, the velocity at the base of the turbulence-dominated part of the inner layer depends on the velocity at the top of the viscous sublayer, which in turn depends on  $\mu$ . The viscosity-dominated part of the profile can be viewed as “anchoring” the turbulence-dominated part of the profile to the bottom, where the velocity is zero by the no-slip condition. So to get the velocity profile we have to start with the velocity gradient, rather than the velocity itself, and write  $d\bar{u}/dy = f(\tau_0, \rho, y)$  in dimensionless form as

$$\frac{y}{u_*} \frac{du}{dy} = A \quad (4.23)$$

where  $A$  is a dimensionless constant that should hold in this particular layer for all turbulent channel flows over smooth boundaries, and then integrate to obtain the dimensionless velocity profile:

$$\frac{\bar{u}}{u_*} = A \ln y + A_1 \quad (4.24)$$

where  $A_1$ , also dimensionless, is a constant of integration. By the concept of Reynolds-number similarity discussed above,  $A$  should be very nearly constant provided that the Reynolds number is high enough for the turbulence to be fully developed.

**101** Note that Equation 4.24 does not contain  $\mu$  explicitly, but from what was said above,  $\mu$  has to be in there somewhere. The resolution of this seeming paradox is that the constant of integration  $A_1$  must depend upon  $\mu$ . You can verify that this is so by noting that Equation 4.24 can be put into the general form of the law of the wall given by Equation 4.17 if and only if  $A_1$  is equal to  $A \ln(\rho u_* / \mu) + B$ : putting this expression for  $A_1$  into Equation 4.24,

$$\begin{aligned} \frac{\bar{u}}{u_*} &= A \ln y + A \ln \frac{\rho u_*}{\mu} + B \\ &= A \ln \frac{\rho u_* y}{\mu} + B \end{aligned} \quad (4.25)$$

The constant  $B$  is just the residuum of the constant of integration after  $A \ln(\rho u_* / \mu)$  has been extracted.

**102** There is no universal agreement in the literature on the values of the constants  $A$  and  $B$ :  $A$  is usually taken to be between 2.4 and 2.5, and  $B$  is taken to be between 5 and 6. The small differences in  $A$  and the larger differences in  $B$  from source to source are an understandable result of fitting straight lines in semilogarithmic plots of slightly scattered data from diverse experimental studies. Discussions on the values of these constants can be found in Monin and Yaglom (1971) and Hinze (1975). With the commonly used values  $A = 2.5$ ,  $B = 5.1$ , Equation 4.25 becomes

$$\frac{\bar{u}}{u_*} = 2.5 \ln \frac{\rho u_* y}{\mu} + 5.1 \quad (4.26)$$

**103** The constant  $A$ , which is a reflection of the nature of turbulent momentum transport in the inner layer, is often written  $1/\kappa$ , and  $\kappa$  is called *von Kármán's constant*. Thus,  $\kappa$  has a value very nearly 0.4. The reason  $A$  is written as  $1/\kappa$  is historical, not fundamental. Also, you should expect a weak dependence of  $A$  on the mean-flow Reynolds number. The exact nature of variation of  $A$  with the Reynolds number, and with the suspended-sediment concentration in sediment-transporting flows as well, has been controversial.

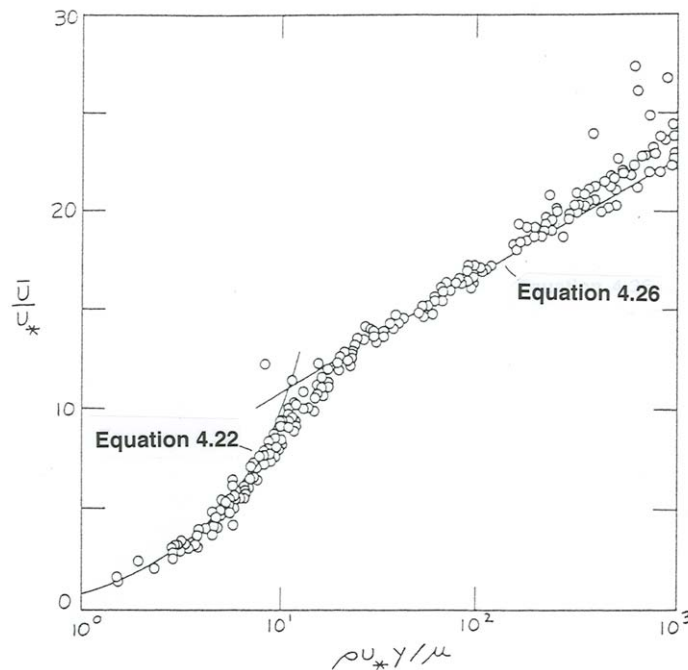


Figure 4-26. Plot of dimensionless mean flow velocity  $\bar{u}/u_*$  vs. dimensionless distance from the boundary,  $\rho u_* y/\mu$ , for the inner layer over a smooth boundary in turbulent open-channel flow. This plot represents the law of the wall for dynamically smooth flow.

**104** Equation 4.26 shows that the velocity profile is expressed by a single curve for the turbulence-dominated part of the inner layer, just as was the case for the viscosity-dominated part. It is the profile given by Equation 4.26 that is usually called the law of the wall, although that term more properly describes the whole inner-layer profile, viscosity-dominated and turbulence-dominated, plus the transition between.

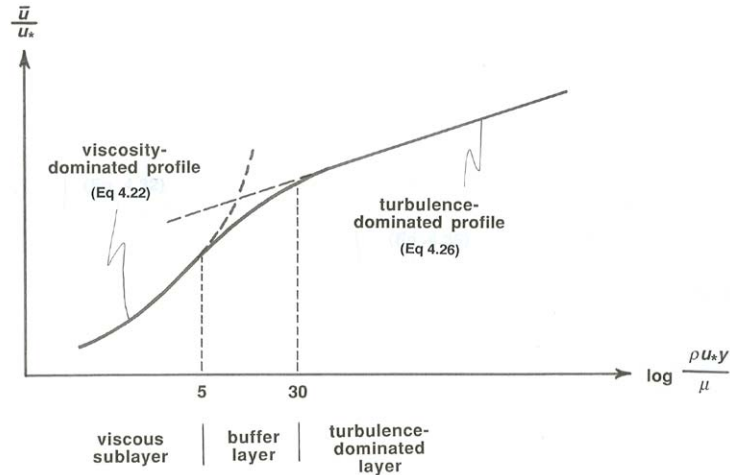


Figure 4-27. Schematic version of Figure 4-26.

**105** In summary, time-average velocity  $\bar{u}$  in the inner layer over a smooth boundary, when nondimensionalized by dividing by  $u_*$ , should plot as a single curve as a function of  $y^+$ , the dimensionless distance above the bottom. Figure 4-26, which incorporates the data already plotted in Figure 4-25 for the viscous sublayer, shows the velocity profile through the whole of the inner layer over a smooth boundary. This profile represents the complete law of the wall for smooth boundaries. The data points in the viscosity-dominated part of the inner layer follow Equation (4.22); the data points in the turbulence-dominated part of the inner layer follow Equation (4.26), which plots here as a straight line because of the semilogarithmic coordinates.

**106** Between  $y^+$  values of about 5 and about 30 in Figure 4-26 there is a smooth transition between the viscosity-dominated profile (Equation 4.22) and the turbulence-dominated profile (Equation 4.26); see Figure 4-27. This is the buffer layer, where viscous shear stress and turbulent shear stress are both important. For  $y^+ < 5$  the turbulent shear stress is negligible, and Equation 4.32 describes the profile; for  $y^+ > 30$  the viscous shear stress is negligible, and Equation 4.36 describes the profile. It is in wall-law plots like Figure 4-26 that the lower and upper limits of the buffer layer are most clearly manifested. You will see a variety of lower and upper limiting  $y^+$  values mentioned in the literature; this is understandable, because the divergence of the curves given by Equations 4.22 and 4.26 from the actual profile is gradual. Although it is of no great physical significance, the height of intersection of Equations 4.22 and 4.26 in the buffer layer is at  $y^+ = 11$ , as you can see from Figure 4-26. What is of greater significance is that the turbulent shear stress and the viscous shear

stress are found experimentally to be equal at a slightly larger  $y^+$  value of about 12; this is in a sense the “middle” of the buffer layer.

**107** The dimensionless height  $y^+$  above the boundary at which  $\bar{u}/u_*$  begins to deviate from the law of the wall depends on the mean-flow Reynolds number  $Re$ ; it ranges upward from around 500 at small  $Re$  to over 1000 at larger  $Re$ . For  $y^+$  greater than this,  $\bar{u}/u_*$  is greater than predicted by the law of the wall.

**108** How thick is the inner layer? The upper limit of  $y^+$  for the law of the wall at high Reynolds numbers for open-channel flow is not well established, but assume a  $y^+$  value of 1000 in a flow of room-temperature water 1 m deep at a mean flow velocity of 0.5 m/s. Then  $y$  at the outer limit of the inner layer is about 5 cm. (To figure this out, compute  $Re$ , use the smooth-flow curve in Figure 4-20 to get  $f$  and therefore  $\tau_0$ , and put that into  $y^+$ .) So the inner layer occupies only a small percentage of the flow depth, no more than 10–20%. And the viscous sublayer in this flow is only a fraction of a millimeter thick. Note that the logarithmic abscissa axis in plots like Figure 4-26 crowds the whole outer layer, in which Equation 4.26 no longer holds, into a small part of the graph.

**109** Most of the data points in Figure 4-26 are from flows in circular pipes and rectangular ducts rather than from open-channel flows. But data from open-channel flows, and from boundary layers developing on flat plates as well, are consistent with those from flow in pipes and ducts. This emphasizes the important point that the law of the wall holds for a wide variety of geometries of outer-layer flow. From the earlier discussion of variables important in the inner and outer layers, this should be no surprise: the flow in the inner layer is governed by local effects and is independent of the nature of the outer flow. In fact, the law of the wall is even more general: although we won't pursue the matter here, the law of the wall holds even when there is a substantial pressure gradient (negative or positive) in the direction of flow, resulting in downstream acceleration or deceleration.

---

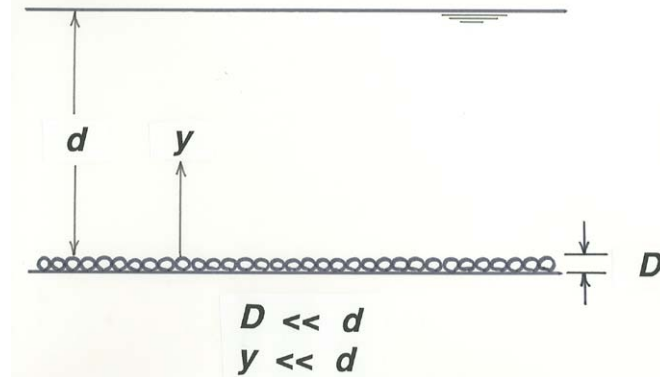


Figure 4-28. Definition sketch for analysis of mean velocity profiles in dynamically rough flow.

### *The Law of the Wall for Rough Boundaries*

**110** In many turbulent boundary-layer flows, the boundary is not physically smooth but instead is occupied by, or is covered by, or consists of, roughness elements of some kind. By the term *roughness element* I mean any local part of the boundary that protrudes above the overall or average boundary surface. Such things as buildings, trees, crops, people, water waves, sand particles, boulders, or corrosion scales come readily to mind. In what follows, we will assume (Figure 4-28) that the roughness elements are much smaller than the flow depth ( $D \ll d$ ) and that the layer of the flow we will consider, for now, has a thickness that is not a large fraction of the flow depth ( $y \ll d$ ). Provided that the roughness elements are not much smaller than the thickness of the viscous sublayer, the velocity profile in the boundary layer depends on the size, shape, and arrangement of the roughness elements as well as on  $\tau_0$ ,  $\rho$ ,  $\mu$ , and  $y$ :

$$\bar{u} = f(\tau_0, \rho, \mu, y, \text{roughness geometry}) \quad (4.27)$$

where the roughness geometry is specified by the size distribution, the shape distribution, and the plan-view packing or arrangement of the roughness elements.

**111** To make any progress we have to be specific about the nature of the roughness. Assume here that the roughness is composed of fairly well sorted mineral sediment particles with the usual natural range of particle shape and roundness, and that the particles form a full sediment bed that is

planar on a large scale. Roughness of this kind, called *close-packed granular roughness* by fluid dynamicists, is fairly well characterized by the single variable  $D$ , the mean or median particle size. This roughness is the best-studied kind, and it is important in a great many natural water flows over sediments, but there are many other kinds of roughness, in both nature and technology.

**112** With the above simplifications, Equation 4.27 becomes

$$\bar{u} = f(\tau_0, \rho, \mu, y, D) \quad (4.28)$$

or, in dimensionless form,

$$\frac{\bar{u}}{u_*} = f\left(\frac{\rho u_* y}{\mu}, \frac{\rho u_* D}{\mu}\right) \quad (4.29)$$

So for flow over rough boundaries the dimensionless velocity  $u/u_*$  generally depends not only on  $y^+$  but also on the boundary Reynolds number. Equation 4.28, which could also be written using  $y/D$  instead of  $\rho u_* y/\mu$ , is called *the law of the wall for granular-rough boundaries*.

**113** Two different aspects of the effect of the roughness on the velocity profile become apparent upon examination of Equation 4.29. First, the size of the roughness elements relative to the thickness of the viscous sublayer is important. Remember from the section on smooth flow and rough flow earlier in this chapter that if  $D$  is much smaller than the viscous length scale  $\mu/\rho u_*$  the roughness elements are embedded in the viscous sublayer, whereas if  $D$  is much larger than  $\mu/\rho u_*$  there is no viscous sublayer and the roughness elements are enveloped in turbulence generated by flow separation around upstream elements. You should suspect, then, that for very small  $\rho u_* D/\mu$  (less than about 5, for which viscous-sublayer thickness and roughness height are about equal), the roughness has no effect on the velocity profile. Under these conditions the velocity profile over physically rough boundaries is indeed found to coincide with that over physically smooth boundaries—provided that we do not place our velocity meter so close to the bed that individual roughness elements distort the velocity field. The law of the wall for smooth boundaries, Equations 4.22 and 4.26 together with the transition between them through the buffer layer, therefore holds for flows with  $\rho u_* D/\mu < 5$  over physically rough boundaries also. These are the flows that in the section on flow resistance were termed dynamically smooth even though physically rough and were shown to fall on the curve for physically smooth boundaries in the resistance diagram in Figure 4-20. For very large  $\rho u_* D/\mu$ , however, there is no viscous sublayer and therefore no effect of  $\mu$  on the velocity profile,

and you should expect to see a velocity profile that is rather different from the law of the wall for smooth flow. The next two subsections are devoted to the velocity profile in these dynamically rough flows.

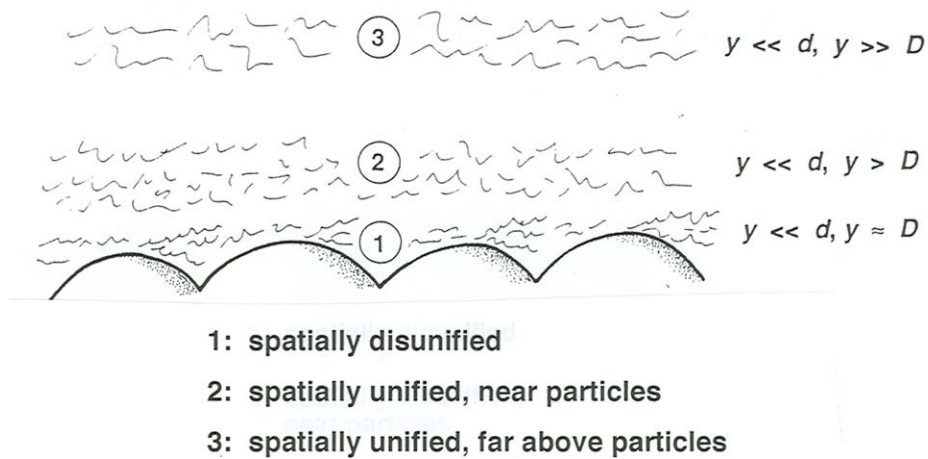


Figure 4-29. Differing regions of flow as a function of distance from the boundary in dynamically rough flow.

**114** Second, in the case of rough flow the value of  $y$  relative to  $D$  is important (Figure 4-29). For  $y \approx D$ , at points in the flow that are nestled among the roughness elements themselves or are just a few roughness heights above the tops of the roughness elements, the velocity depends in a complicated way on the shapes of the roughness elements and on the position of the profile relative to individual elements, and we should not expect to find any generally applicable profile; the velocity profile could be said to be *spatially disunified*. A bit higher in the flow, several diameters above the tops of the elements, the wakes shed by individual elements blend together in such a way that the velocity profile is about the same at all positions, but the flow structure is still affected by the roughness-generated turbulence. Far above the tops of the elements, however, for  $y \gg D$ , it is reasonable to expect that the turbulence structure is governed by local dynamics, as in smooth flow, and not by the wakes from the little roughness elements far below. If  $D$  is sufficiently smaller than the flow depth  $d$ , there should then be a layer of the flow for which  $y \ll d$  and  $y \gg D$  at the same time—that is, a part of the inner layer in which roughness-generated turbulence is not of direct importance. Remember, however, that by analogy with what was said about smooth flow above, this

part of the profile still has to be anchored at its lower end to that part of the velocity profile controlled by the roughness-generated turbulence.

**115** In the following I will present the velocity profile in rough flows for which there is indeed a zone for which  $y \ll d$  but at the same time  $y \gg D$  (or, more precisely, above the near-bed layer of spatial disunification of the profile, which is something like several roughness heights above the tops of the roughness elements). I will deal only with the region far enough above the bed that the roughness elements do not affect the profile shape; this could be called “the inner layer far above the roughness elements”. I will make only a few brief comments about the equally important flows in which there is no zone for which  $y \ll d$  and  $y \gg D$ , examples being shallow flows in gravel-bed streams.

**116** In the part of the inner layer for which  $y \gg D$ , neither  $\mu$  nor  $D$  affects the slope of the velocity profile. We can therefore make exactly the same statement as for the turbulence-dominated part of the inner layer in physically smooth flow: the velocity gradient  $d\bar{u}/dy$  depends only on  $\tau_0$ ,  $\rho$ , and  $y$ . This leads again to Equation 4.23, and upon integration, to Equation 4.24. We should even expect the constant  $A$  to be the same, because it is a manifestation of the vertical turbulent transport of streamwise fluid momentum, and we just concluded that sufficiently far from the boundary the structure of the turbulence depends only on local effects and is independent of the turbulence shed by the boundary roughness. The constant of integration  $A_1$ , however, is *different*, because it depends on the nature of the connecting velocity profile nearer the boundary, which is different from that in smooth flow. This latter difference has to do with the relative importance of viscous shear stress and turbulent shear stress near the boundary, and with the relative importance of viscous drag and pressure drag at the boundary: if  $D \gg \mu/\rho u_*$  (I termed such flows fully rough), viscous shear stress in the flow and viscous drag on the boundary are negligible, so not only the velocity gradient but also the velocity itself is unaffected by  $\mu$  in the layer under consideration here.

**117** We can rearrange Equation 4.24 to obtain Equation 4.25 just as in the case of smooth flow, but with one important difference: by comparison with the general form of the law of the wall for rough flow (Equation 4.29), the term  $B$  is now not a constant but instead a function of the boundary Reynolds number:

$$\frac{\bar{u}}{u_*} = A \ln \frac{\rho u_* y}{\mu} + f\left(\frac{\rho u_* D}{\mu}\right) \quad (4.30)$$

**118** Equation 4.30 can be put into an equivalent but more revealing and more useful form by splitting  $f(\rho u_* D/\mu)$  into two parts:  $-A \ln(\rho u_* D/\mu)$  plus a remainder that is some different function of  $\rho u_* D/\mu$ , which I will call  $B'$ . The only reason for this otherwise arbitrary choice is that now Equation 4.30 can be written

$$\begin{aligned} \frac{\bar{u}}{u_*} &= A \left( \ln \frac{\rho u_* y}{\mu} - \ln \frac{\rho u_* D}{\mu} \right) + B' \\ &= A \ln \frac{y}{D} + B' \end{aligned} \quad (4.31)$$

**119** Equation 4.31 is neater than Equation 4.30, but remember that  $B'$  is a function of  $\rho u_* D/\mu$ . If  $\rho u_* D/\mu$  is sufficiently large, however, so that  $D$  is large relative to what the viscous-sublayer thickness would be, turbulence extends down among the roughness elements and there is no viscosity-dominated layer next to the bottom. The velocity profile then cannot depend on  $\mu$  and therefore not on  $\rho u_* D/\mu$ , so  $B'$  in Equation 4.31 is a constant, which has a value of about 8.5 for uniform, close-packed sand-grain roughness. (There is about as much uncertainty about this constant as there is about the constant  $B$  in Equation 4.25.) The value of  $B$  has indeed been found experimentally to become constant for  $\rho u_* D/\mu > 60$ . It is under these conditions that the flow was termed fully rough in the earlier section on flow resistance. Equation 4.31 can then be written as Equation 4.32, *the law of the wall for fully rough flow*:

$$\frac{\bar{u}}{u_*} = 2.5 \ln \frac{y}{D} + 8.5 \quad (4.32)$$

**120** Figure 4-30 shows Equation 4.32 together with the data from Nikuradse (1933) on which the value of 8.5 for  $B'$  was originally derived. Nikuradse's data were obtained for a particular geometry of granular roughness manufactured by gluing a somewhat open monolayer of subrounded and almost single-size sand to the inner walls of circular pipes. You should expect the value of  $B'$  to be different for different roughness geometries, even if the average roughness height is the same, because the shape and arrangement of the roughness elements would be different, and this affects the details of the turbulence structure right near the boundary and thus also the velocity profile right near the boundary.

---

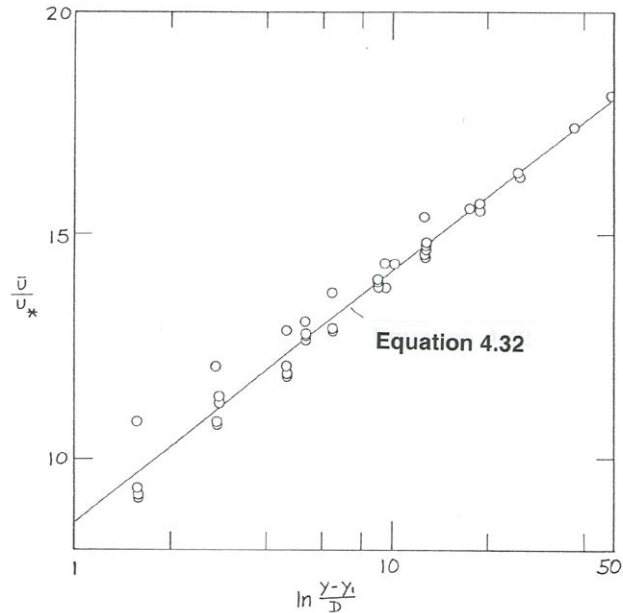


Figure 4-30. Plot of  $\bar{u}/u_*$  vs.  $y/D$  for the inner layer over granular-rough boundaries. Data are from Nikuradse (1933) for runs with pipe radius  $> 60D$ . Only data for which  $Re^* > 60$  are shown, so this plot represents the law of the wall for dynamically fully rough flow. All points up to 0.2 times the pipe radius are shown. Included are eight profiles from four sand-lined pipes. As described in a later section, the  $y = 0$  level has been adjusted downward from the tops of the grains a distance  $y/D = -0.36$  to extend the straight-line fit as close to the bed as possible.

---

**121** Figure 4-31 is another plot of Equation 4.32, this time without the data points. It is meant to serve as a warning about how close to the boundary Equation 4.32 actually applies. Recall that at heights no greater than a few roughness-element sizes, the flow can be said to be spatially disunified (see Paragraph 114 above), and in that region the basis for derivation of Equation 4-32 no longer holds. That is emphasized, in cartoon form, by the blurring of the profile near the rough boundary.

---

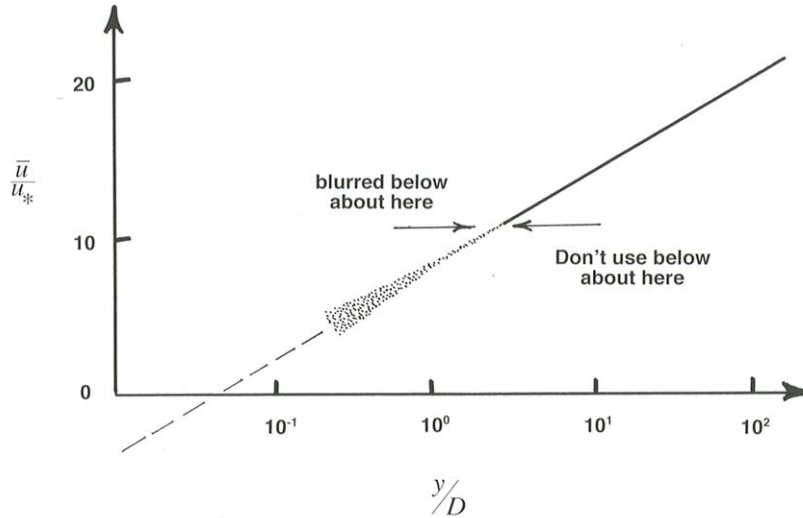


Figure 4-31. Plot of  $\bar{u}/u_*$  vs.  $y/D$  for the inner layer over granular-rough boundaries (Equation 4.32), showing the region near the bed where the profile fails to follow Equation 4.42.

**122** As is commonly done, you can preserve the value of 8.5 for  $B'$  in Equation 4.31 and use for  $D$  the fictitious diameter of single-size sand grains in a uniform monolayer that makes Equation 4.31 fit the velocity data best. That size is called the *equivalent sand roughness*, usually denoted  $k_s$ . (A more descriptive term would be the “equivalent Nikuradse-style sand roughness”.) In other words,  $k_s$  for any given bed roughness, of any kind whatever, is the uniform-sand-grain height that gives the same wall-law velocity distribution for a given value of  $\tau_0$ . On the face of it this seems like a neat way around the problem of what the value of  $B'$  is, but keep in mind that to determine  $B'$  in the first place you need to measure both the velocity profile and the boundary shear stress, independently, at the same time.

**123** For  $5 < \rho u_* D / \mu < 60$  the flow is said to be *transitionally rough*. The velocity profile is still a semilog straight line for  $y \gg D$ , whether  $\bar{u}/u_*$  is plotted against  $\rho u_* y / \mu$  as in Figure 4-26 or against  $y/D$  as in Figure 4-30, and it still has the same slope given by the universal constant  $A$ . But the position of the straight line varies as the near-bed part of the profile changes from the smooth-flow profile shown in Figure 4-26 to the fully rough profile shown in Figure 4-30. For transitionally rough flows, the law of the wall in the innermost region, where there is some dependence on  $\mu$ , cannot be derived in the form of a simple equation like Equation 4.26 or

Equation 4.31; keep in mind, however, that some form of the general law of the wall for rough boundaries (Equation 4.30) holds there nonetheless.

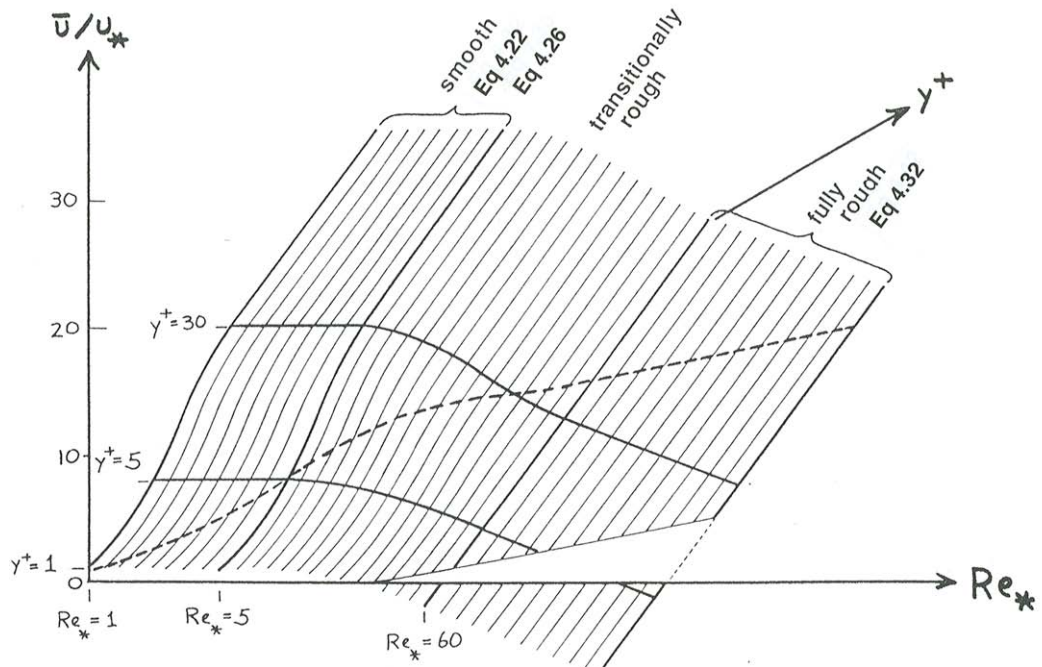


Figure 4-32. Combined plots of the law of the wall in smooth, transitionally rough, and fully rough flows.

**124** Finally, if  $\rho u_* D / \mu$  is very small the roughness elements are deeply embedded in the viscous sublayer and can have no effect on the structure of the turbulence and the shape of the velocity profile above the viscous sublayer. The velocity profile is then the same as if the boundary were physically smooth. As discussed earlier in the section on flow resistance, the flow is dynamically smooth even though physically rough.

**125** Figure 4-32, a combined plot of the law of the wall in smooth and rough flows, summarizes much of what is in this section and the previous one (see also Figure 4-33). The three-dimensional surface in Figure 4-32, drawn by use of Equations 4.22, 4.26, and 4.32, shows  $\bar{u}/u_*$  as a function of  $y^+$  and  $Re_*$ . In smooth flows, represented by the left-hand part of the surface, the velocity profiles do not depend on  $Re_*$ , so the surface is a cylinder whose elements are parallel to the  $Re_*$  axis. Each of the several profiles shown, which represent intersections of the surface with planes for which  $Re_* = \text{const}$ , is exactly the same as that in Figure 4-26. In

fully rough flows, represented by the region to the right of the plane  $Re_* = 60$ , the velocity profiles depend only on  $y/D$ . To see why the right-

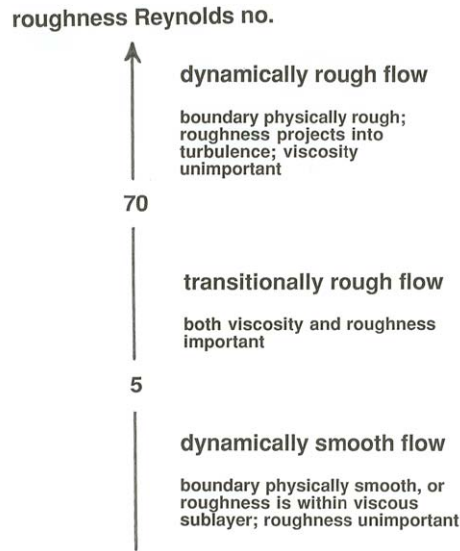


Figure 4-33. Ranges of roughness Reynolds number for dynamically smooth flows, transitionally rough flows, and fully rough flows.

hand part of the surface slopes downward to the right, write  $\ln(y/D)$  as  $\ln(\rho u_* y / \mu) - \ln(\rho u_* D / \mu)$ , or  $\ln y^+ - \ln Re_*$ ; thus, the larger the value of  $Re_*$ , the smaller the value of  $\bar{u} / u_*$  for a given value of  $y^+$ . Because there is no viscous sublayer or buffer layer to contend with, the profiles are straight lines all the way down to positions not far above the tops of the roughness elements. The rough-wall profile deviates from a semilog straight line within several roughness heights above the tops of the roughness elements—to say nothing of the spatial disuniformity of the velocity profile that sets in at a level just above the tops of the roughness elements. Only at points on the surface in Figure 4-32 well above the dashed curve that expresses the condition  $y = D$  are the profiles valid; the part of the surface shown in the lower right is therefore useful only hypothetically, for displaying the nature of the relationships. Finally, in the middle part of the surface the profiles are transitional between the smooth and the fully rough profiles. Here the lines for  $y^+ = 5$  and  $y^+ = 30$  shown on the left-hand part of the surface lose their physical significance as the viscous sublayer disappears.

**126** Note in Figure 4-32 that at any value of  $y^+$  well up in the inner layer  $\bar{u}/u_*$  in any rough flow is less than  $\bar{u}/u_*$  in any smooth flow, although the slopes of the profiles for the two flows are the same at that height. This is because nearer the bottom the velocity increases more sharply with distance from the bottom in smooth flow than in rough flow. Figure 4-34 shows that effect, in cartoon form: the profile for rough flow lies everywhere below the profile for smooth flow. You can think of the two profiles shown in Figure 4-34 as being representative of the left and right extremes of the surface shown in Figure 4-32, given that the surface slopes downward to the right in Figure 4-32.

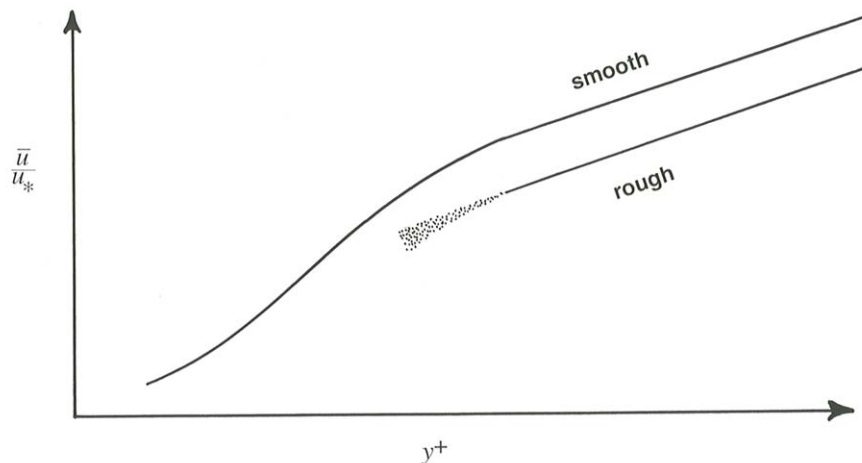


Figure 4-34. Cartoon plot showing the comparison between velocity profiles for smooth flow and rough flow.

**127** A conventional additional step that is taken with Equation 4.31 is to write  $B'$  in the form  $-A \ln(y_0/D)$ , where the quantity  $y_0$ , with the dimensions of length, is called the **roughness length**. (Outdoors fluid dynamicists like meteorologists take the normal-to-boundary coordinate direction to be  $z$ , so they deal with  $z_0$ , not  $y_0$ .) Note: if you read the literature on velocity profiles in natural flow environments, you are likely to encounter this roughness length, rather than the equivalent quantities I have used earlier in this section.

**128** Use of  $y_0$  allows  $B'$  to be completely absorbed into the log term in Equation 4.32:

$$\begin{aligned}\frac{\bar{u}}{u_*} &= A \ln \frac{y}{D} - A \ln \frac{y_0}{D} \\ &= A \ln \frac{y}{y_0}\end{aligned}\tag{4.33}$$

By the definition of the natural logarithm,  $y_0$  can be written in terms of  $B'$  as  $y_0 = D \exp(-B'/A)$ .

**129** If the flow is only transitionally rough,  $y_0$  is a function of  $\rho u_* D / \mu$ , as is  $B'$ . If the flow is fully rough, however,  $y_0$  is independent of  $\rho u_* D / \mu$  for the same reason that  $B'$  in Equation 4.30 is independent of  $\rho u_* D / \mu$ . Warning: don't confuse  $y_0$  with the actual roughness height  $D$ : for a given geometry of roughness in fully rough flow  $y_0$  is proportional to  $D$  (for close-packed uniform sand-grain roughness  $y_0 = D/30$ ), but the proportionality coefficient varies considerably depending upon the particular geometry of the roughness.

**130** Setting  $y$  equal to  $y_0$  in Equation 4.33 gives  $\bar{u}/u_* = 0$ . So another way of looking at  $y_0$  is that it is the height at which the velocity would become zero if the logarithmic rough-wall equation for the velocity profile could be extended down to that height. It is important to remember, however, that Equation 4.33 becomes inapplicable far above that position, which is nestled in among the roughness elements. (That is why I used the contrary-to-fact “subjunctive” verb construction in the preceding sentence.) See the very brief comments in the next paragraph.

**131** We still have not considered the lowermost part of the inner layer, not far above the tops of the roughness elements. For sand-size bed roughness this region is not much more than a few millimeters thick, but for water flowing over gravels or for wind blowing over large ground-surface roughness like buildings or vegetation it may be decimeters or even meters thick, and no sophisticated, miniaturized velocity meters are needed to include it in measured velocity profiles. At positions this close to the bed, two complications arise: the logarithmic profile becomes distorted, and there is no obvious choice for  $y = 0$ .

### *Velocity Defect Law*

**132** Now look at the velocity profile in the outer layer. There the velocity is most naturally specified relative to that at the boundary with the free stream (or, in the case of free-surface flow, relative to the surface velocity, or in the case of pipe flow, relative to the centerline velocity), because we have seen that the inner layer, with a different relationship for the velocity, intervenes between the outer layer and the bottom boundary.

In other words, if we look at the velocity relative to that at the surface we do not have to worry about how the velocity is anchored to the bottom through the inner layer. So instead of  $\bar{u}$  we use  $U_s - \bar{u}$ , called the **velocity defect**, where  $U_s$  is the surface (i.e., maximum) velocity.

**133** If you go back and review the discussion in the section on inner and outer layers you will see that the structure of the turbulence in the outer layer should depend on  $\tau_o$ ,  $\rho$ ,  $y$ , and  $d$ , but not on  $\mu$ , for the same reason that the velocity profile in the turbulence-dominated part of the inner layer does not depend on  $\mu$ . Because this is true from the free surface down to the bottom of the outer layer, and because  $U_s - \bar{u}$  characterizes the velocity relative to the free surface rather than the bottom, then not just the velocity gradient  $d\bar{u}/dy$  (as in the turbulent part of the inner layer) but also  $U_s - \bar{u}$  itself is independent of  $\mu$ . Turbulence structure and  $U_s - \bar{u}$  should not depend on  $D$  either, provided that  $D \ll d$ . So the general form of the velocity-defect profile is

$$U_s - \bar{u} = f(\tau_o, \rho, y, d) \quad (4.34)$$

or in dimensionless form

$$\frac{U_s - \bar{u}}{u_*} = f\left(\frac{y}{d}\right) \quad (4.35)$$

**134** Equation 4.35 tells us that the dimensionless velocity defect depends only on the dimensionless height above the bottom. This relationship for the velocity profile in the outer layer is called the **velocity-defect law**. I will defer further discussion of velocity profiles in the outer part of the flow until the following section, where an examination of the region of overlap between the inner and outer layers affords further insight into the form of the velocity-defect law.

#### *The Overlap Layer; More on the Velocity-Defect Law*

**135** One more matter to consider in this exposition of velocity profiles has to do with the **overlap layer**, where at sufficiently high mean-flow Reynolds numbers the conditions defining the inner and outer layers hold simultaneously; I refer you once more to the earlier section on inner and outer layers. This overlap layer is far enough from the bottom that the flow structure is independent of both viscosity and the characteristics of the bottom roughness but close enough to the bottom that the flow structure is independent of the flow depth (Figure 4-35). Here the inner-layer and

outer-layer velocity profiles must *match*—that is, the velocities given by the law of the wall and by the velocity-defect law at any level in the overlap layer must be the same. The upper limit of the overlap layer is at the top of the inner layer. In smooth flow the lower limit is at the top of the buffer layer. With regard to the lower limit in rough flow, presumably the velocity-defect representation of the velocity profile, which looks downward from the free surface and can ignore the details of the bottom roughness, must start to break down when it reaches the lower part of the inner layer, where you have seen that the roughness causes the inner-layer profile to curve away from a semilog straight line.

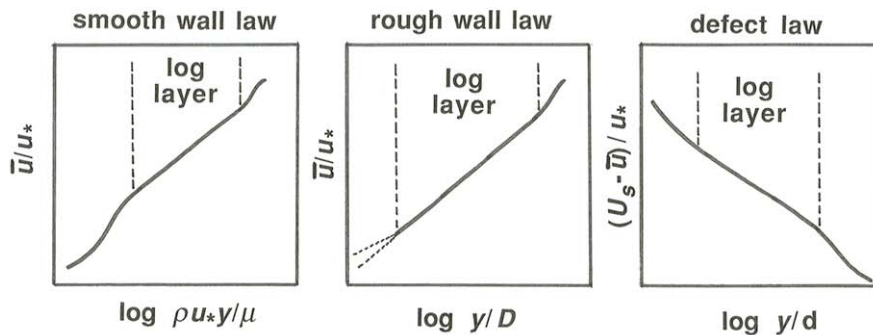


Figure 4-35. The overlap layer (the logarithmic layer) for smooth wall law, rough wall law, and velocity defect law.

**136** The constraints imposed by the matching requirement on the form of both the wall law and the velocity-defect law in the overlap layer were first perceived by Izakson (1937) and Millikan (1939). The mathematical consequence of this matching, which I will not detail here, is that in the overlap layer—but not farther out, beyond the inner layer—the velocity-defect law as well as the wall law is of logarithmic form. The overlap layer is often called the *logarithmic layer*, because in it both the wall law and the defect law are logarithmic.

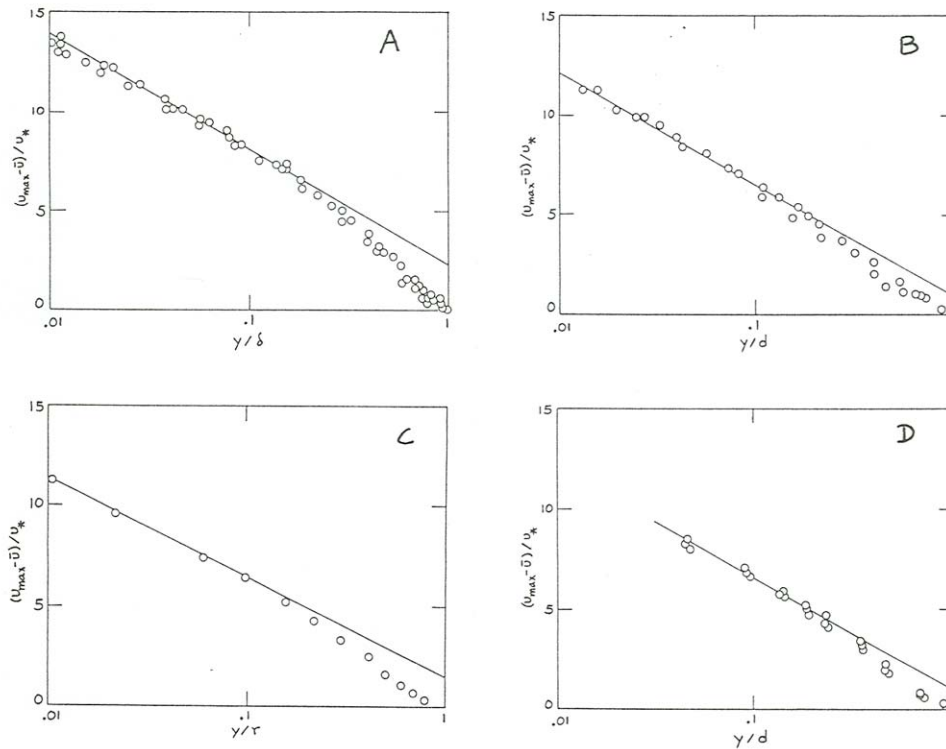


Figure 4-36. Velocity-defect profiles: plots of  $(U_s - \bar{u})/u_*$  versus  $y/D$  in boundary-layer flows with four geometries: **A)** flat plate; **B)** circular pipe; **C)** wide planar duct; and **D)** open-channel flow. After Monin and Yaglom (1971) (various sources), and Coleman (1981). Straight lines with slopes of  $-A$  ( $= -1/\kappa$ ) are fitted to points for  $y/d < 0.2$ .

**137** Figure 4-36 shows velocity-defect profiles on flat plates and in pipes, wide planar ducts, and open channels. The open-channel data, from Coleman (1981), are for a width-to-depth ratio of only about 2, but I have not been able to find any better data; the scarcity of good published data on complete velocity profiles from surface to bottom in steady uniform open-channel flows at large ratios of width to depth is striking. In each graph in Figure 4-36 the data points define a single curve that holds for a wide range of mean-flow Reynolds numbers, indicating that our assumptions about the controls on velocity and turbulence in the outer layer are justified. In each graph there is a well-defined semilog straight-line segment for fairly small  $y/d$ ; that is the log layer. Toward the position of maximum velocity at  $y/d = 1$  the profile breaks away from the semilog straight line to reach the point  $(U_s - \bar{u})/u_* = 0$  at the position of maximum velocity.

**138** The differing shape of the outer part of the velocity-defect profile in different geometries of flow is to be expected because of differing physical effects in the movement and geometry of large eddies in the region of the flow farthest from the solid boundary. Because the outer edge of a freely growing turbulent boundary layer is highly irregular in shape (Chapter 3), at any point near the outer edge passage of large turbulent eddies alternates with passage of nonturbulent fluid, so the efficacy of turbulent momentum exchange is less and the velocity gradient correspondingly steeper than in regions closer to the boundary; this explains the large divergence of the profile from the semilog straight-line segment in Figure 4-36A. In pipes and planar ducts the similar but smaller divergence might be explained by the free passage of large eddies across the centerline or center plane from the opposite sides of the flow. In open-channel flow a similar effect might be produced by flattening of large eddies moving toward the free surface. The meager data from open channels suggest an effect similar in magnitude to that in pipes and planar ducts, or perhaps even smaller. There seems to be no reason to expect a perfectly logarithmic profile all the way to the free surface, but the deviations clearly are insubstantial, at least for practical work.

#### *Effects of Roughness Height and Spacing*

**139** It is in some ways discouraging to sit back and consider that just about everything said so far about velocity profiles is limited to the case of sediment-free flow over close-packed roughness elements

whose size is a tiny fraction of the flow depth. Obviously this is only a small subset of turbulent boundary-layer flows over rough boundaries. The discussion in this section emphasizes mostly the qualitative effects to be expected as (1) the height of the roughness elements increases relative to the flow depth and (2) the spacing of the roughness elements increases relative to their height.

**140** Figure 4-37 summarizes the changes in velocity profile as the size of close-packed granular roughness increases relative to flow depth. In Figure 4-37A the particles are so small (or, more precisely, the roughness Reynolds number  $\rho u_* D / \mu$  is so small) that the particles are embedded in a viscous sublayer, and the flow is dynamically smooth. In Figure 4-37B the particles are larger and the flow is dynamically rough, but the particle size is still so small relative to the flow depth that there is a well developed outer layer beyond the overlap layer in which the velocity-defect profile holds but the inner-layer profile does not. These first two cases are covered by the preceding detailed treatment of velocity profiles.

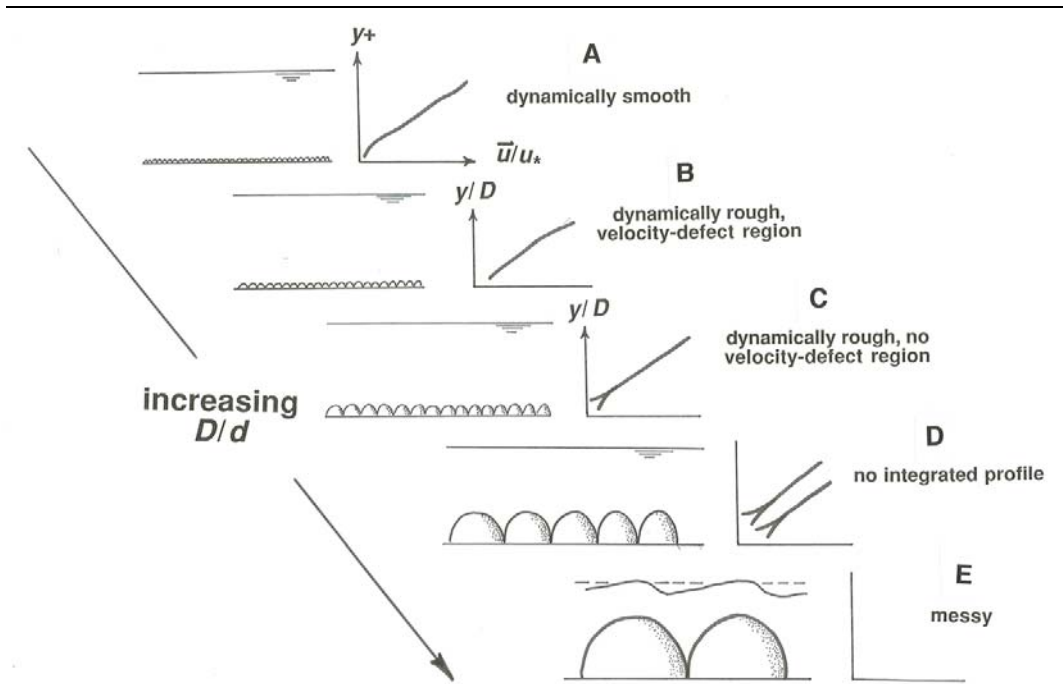


Figure 4-37. Changes in velocity profile as the size of the close-packed granular roughness increases relative to flow depth.

**141** In Figure 4-37C, as the ratio of flow depth to particle size decreases still further, the distinction between inner and outer layers begins to be blurred, and eventually a situation is reached where the entire profile, from bottom to free surface, is affected by the details of the roughness. The whole profile then looks like just the lower part of the wall-law profile in flows with very large values of  $d/D$ . This effect begins to become appreciable at  $d/D$  values of something like 10 to 15.

**142** As  $d/D$  decreases further, an increasingly large fraction of the total flow depth is occupied by the zone of the flow, within one or perhaps two grain diameters above the tops of the roughness particles, where the velocity profile is spatially disunified, in the sense that it varies with position relative to the layout of the particles. As shown in Figure 4-37D in exaggerated form, for  $d/D$  values below about 2 or 3 most or all of the velocity profile is spatially variable in this way.

**143** What happens as  $d/D$  decreases further (Figure 4-37E) depends on the value of the mean-flow Froude number  $U/(gD)^{1/2}$ . (For full

appreciation of this point you will have to wait until I have presented more about free-surface flow later, in the next chapter.) For Froude numbers close to or greater than one (i.e., for supercritical or nearly supercritical flow), the free surface is strongly deformed by the presence of the particles just below the surface; think of a shallow fast-flowing mountain stream with a bed of cobbles and boulders. For the same very small  $d/D$  but low Froude numbers, however, the grains rest just beneath a relatively placid water surface, or in the extreme case project above the surface as islands.

**144** Figure 4-38 is a cartoon showing the changes in the structure of the flow as the roughness spacing decreases relative to the roughness height. Start with a physically smooth and planar bottom; the flow is dynamically smooth, and  $y = 0$  is naturally taken at the planar bottom. Now take a set of roughness elements whose heights are a very small fraction of the flow depth and begin to place them either randomly or in a regular pattern on the bed. The elements could be three-dimensional bluff bodies or two-dimensional ridges transverse to the flow; the effects are qualitatively the same, at least until the ratio of spacing to height becomes very small.

**145** Provided that the roughness Reynolds number (based on the height of the roughness elements being added) is sufficiently large, each element creates a wake as the flow separates around it. From the discussion of flow separation in Chapter 3 you can see that the flow structure downstream of each roughness element is very complicated: the smooth-flow boundary layer is profoundly modified by the development of a highly turbulent shear layer that extends downstream from the separation point. Downstream from each element the flow gradually readjusts toward the boundary-layer structure that would exist in the absence of roughness; the wakes shed by the elements are said to *relax*. This readjustment or relaxation takes the form of a new lowest layer of the flow, expanding upward at the expense of the turbulent shear layer, in which a turbulence-dominated wall-law profile is established in just the same way as in a boundary layer growing on a flat plate. It takes a surprisingly large number of element heights downstream, something of the order of a hundred, for the process to be completed, whereupon the local structure of the flow shows no trace of the presence of the roughness element upstream and the wall-law layer extends without interruption from the planar bottom up into the region of the flow far above the level of the tops of the large roughness elements. The case of low roughness Reynolds numbers is of less interest here, because then the elements are embedded in a viscous sublayer, but in that case also a deficit in fluid momentum is created downstream of each element even though the flow does not separate, and this deficit is ironed

out downstream by viscous shear until the original viscosity-dominated velocity profile is reestablished.

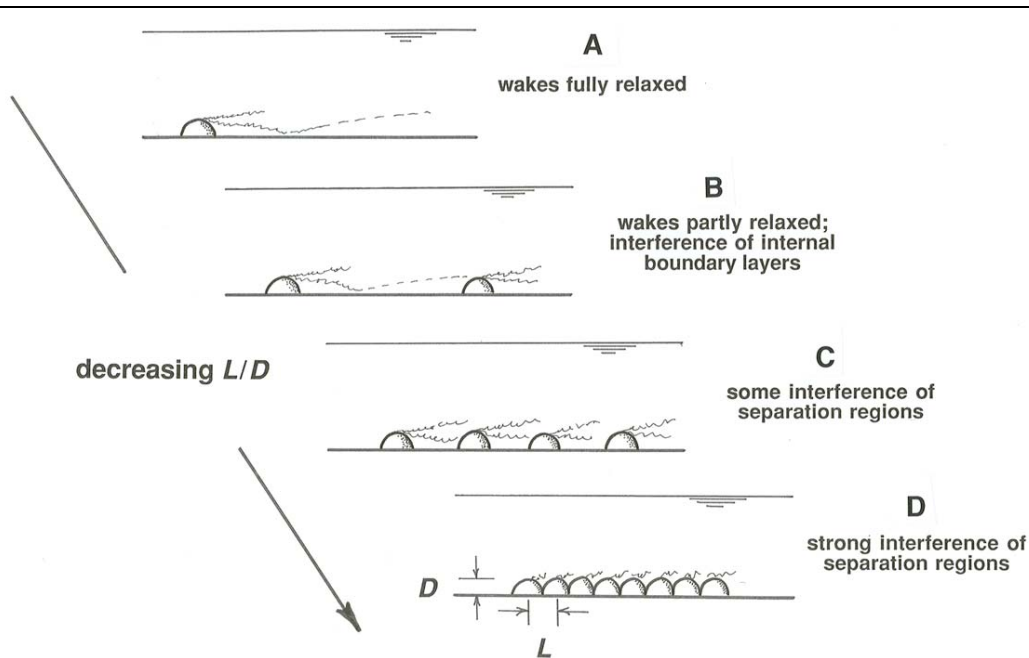


Figure 4-38. Changes in flow structure as roughness spacing decreases relative to roughness height.

**146** If the roughness elements are sufficiently far apart (Figure 4-38A) each has a long wake extending downstream, but the flow is able to return to normal before it encounters the next roughness element. This has been called *isolated-roughness flow* (Morris, 1955). The velocity profile measured above a given point on the bed depends on the position of that point relative to the wakes behind the elements. You would have to measure a large number of profiles and average them spatially to obtain a profile that represents the entire flow. Compared with the original smooth-flow profile before emplacement of any roughness elements, the spatially averaged profile shows a deficit of velocity within one or two roughness heights of the bed.

**147** The spatially averaged boundary shear stress  $\tau_0$  is still dominantly viscous, as in the absence of roughness elements, but the contribution of pressure drag to  $\tau_0$  increases with the roughness density. The flow could now be termed transitionally rough, although in a rather

different sense from the use of that term in flow over close-packed roughness in earlier sections. Note also that the original flow, before emplacement of roughness elements, can itself be dynamically rough, if the bottom is covered with close-packed roughness that is much smaller than the large, isolated roughness we are adding. Then  $\tau_0$  is dominated from the start by pressure drag, but this pressure drag is of two parts: a spatially uniform part produced by the underlying small and close-packed roughness, and a spatially nonuniform part produced by the large and isolated roughness. It takes only a low density of large roughness elements for their contribution to the pressure drag to outweigh that of the close-packed elements.

**148** As we continue to add large roughness elements, a point is reached where the wakes shed by the elements do not relax completely before encountering another roughness element downstream, and with some further increase in density most points in the near-bed flow are within wakes in various stages of relaxation (Figure 4-38B). Now there is no place on the bed that shows the relatively simple velocity profile of the original smooth flow without roughness elements. A flow of this kind has been called *wake-interference flow* (Morris, 1955). Again you have to take a large number of local velocity profiles and spatially average them to get a profile representative of the entire bed. Because most of the area of the bed is overlain by reattached and relaxing wakes, the spatially averaged profile shows two distinct segments: one, adjacent to the bed and extending upward for some fraction of the roughness height, represents the spatial average of the local wall-law profiles in the relaxing wakes, and the other, starting well above the tops of the large roughness elements and extending far above, represents the wall law above the zone in which the upward-diffusing wake turbulence blends into a spatially uniform layer—the case that was treated at length in the earlier part of this chapter. These two distinctive parts of the profile tend to plot as semilog straight lines with a transition at heights somewhat below to somewhat above the tops of the roughness elements. See Nowell and Church (1979) for a good example. As the roughness spacing decreases, the height of the  $y = 0$  level for the overall wall-law profile above the tops of the roughness elements rises higher and higher above the planar bottom.

**149** With increasing roughness density, eventually most of the area of the bed between roughness elements is overlain by the parts of the wakes that lie upstream rather than downstream of reattachment (Figures 4-38C, 38D); this condition sets in when the ratio of roughness spacing to roughness height is of the order of ten or less. Well before this stage the lower straight-line segment of the spatially averaged velocity profile loses its distinctive character. The turbulent shear layers downstream of loci of

separation then impinge mostly upon the surfaces of roughness elements downstream rather than on the planar bottom; viscous shear stresses on the planar bottom are almost nonexistent, and the geometry of the bottom in the areas between the roughness elements is irrelevant to the dynamics of the flow. For three-dimensional granular roughness this condition is maintained with no qualitative change as the elements become so closely spaced that their bases are touching—a good approximation to the condition of a loose granular bed treated in detail earlier. If the roughness consists of transverse ridges, however, the ratio of spacing to height can continue to decrease toward zero, and as it becomes smaller than about one the flow skims across the crests of the ridges and drives a circulation of stable vortices located in the deep and narrow troughs between the ridges; this has been called *skimming flow* (Morris, 1955).

### **MORE ON THE STRUCTURE OF TURBULENT BOUNDARY LAYERS: COHERENT STRUCTURES IN TURBULENT SHEAR FLOW**

**150** There was a time, until the 1960s, when the emphasis in turbulence research was statistical: turbulence was largely viewed as a strictly *random phenomenon*, one that can be analyzed only by statistical methods. Implicit in such an approach is that turbulence has no apparent regularity or “ordered-ness” in its structure.

**151** Beginning in the 1960s, however, there have been many studies on what are now termed *coherent structures* in turbulent shear flow. (I postponed this material until now, so that you would have more background in turbulent shear flow to bring to it.) It has become clear that shear turbulence is not merely a random assemblage of eddies of all sizes, shapes, and magnitudes and orientations of vorticity; rather, these are irregular but repetitive eddy structures, or flow patterns, in time and space, with distinctive shapes and histories of formation, evolution, and dissipation. These coherent structures are not strictly regular in geometry or periodic in time, but nonetheless they have a strong and distinctive element of non-randomness. One way of describing these coherent structures is that they are quasi-regular, or quasi-periodic, or quasi-deterministic. (The word *quasi* in Latin means “almost”.) Admittedly the foregoing characterization does not give you much basis for imagining or visualizing what the coherent structures look like; see below for more concrete material.

**152** Recall from Chapter 3 that turbulence can be viewed as an assemblage of swirling and intergrading parcels of fluid, called eddies, on a wide range of scales. Eddies have *vorticity*: the fluid in the eddies undergoes rotational motion, which is described by the local rate and

orientation of rotation, varying from continuously from point to point. To appreciate the nature of coherent structures in shear turbulence, you need to deal with the shapes and also the vorticity of the structures, and how the shape and the vorticity develop and change during the lifetime of a given element of structure.

**153** The best way to perceive or capture ordered structures is to visualize them, by supplying the flow with marker material that reveals or distinguishes differently moving regions of fluid. Studies of ordered structures in turbulent flow have mostly used three techniques flow visualization:

- dye injection, at points or along lines
- generation of lines of tiny hydrogen bubbles in water by passing a current through a fine platinum wire immersed in the flow
- high-speed motion-picture photography of very small opaque solid particles suspended in the flow

**154** It is generally agreed that flow near the boundary in a turbulent shear flow tends to be characterized by the following sequence of events, commonly called the *burst-sweep cycle*. A high-velocity eddy or vortex (called a *sweep*) moves toward the boundary and interacts with low velocity fluid near the boundary to cause acceleration, increase in shear, and development of small-scale turbulence; this accelerated fluid is then lifted from the boundary and ejected as a turbulent *burst* into a region of flow farther from the boundary. The sweeps are intrusions of high-speed fluid at a shallow angle toward the wall; the bursts are violent ejections of low-speed fluid outward from the vicinity of the wall.

**155** Close to the boundary the high-velocity and low-velocity vortices or eddies tend to be elongated or streaked out in the streamwise direction, and their manifestation is a streaky or ribbon-like pattern of high and low fluid velocities, and therefore of boundary shear stresses as well. Owing to the substantial changes in velocity, shear, and turbulence above a given point on the boundary occasioned by the bursting cycle, the effective thickness of the viscous sublayer varies with time. Because of the existence of the burst-sweep cycle, the picture of the viscous sublayer developed earlier in this chapter is oversimplified: it has a definite thickness only as a time average at a given point. At a given time, the viscosity-dominated layer near the bottom is in some regions thin (and in those regions, shear near the bed, and shear stress on the bed, are

temporarily high), and in adjacent regions it is thicker (and in those regions, the shear and the bed shear stress are temporarily smaller).

---

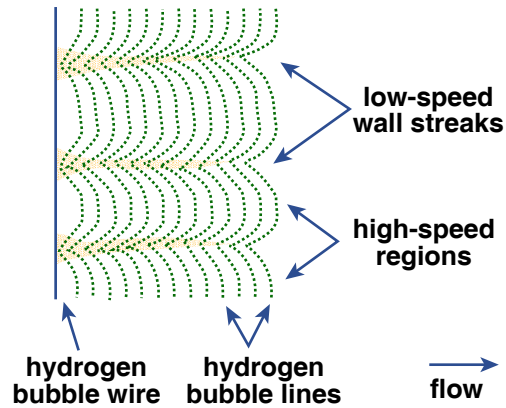


Figure by MIT OpenCourseWare.

Figure 4-39. Low-speed wall streaks and high-speed regions, as seen from above, revealed by the distortion of a horizontal cross-stream line of hydrogen bubbles generated along the left-hand line just above the wall. (From Smith, 1996.)

---

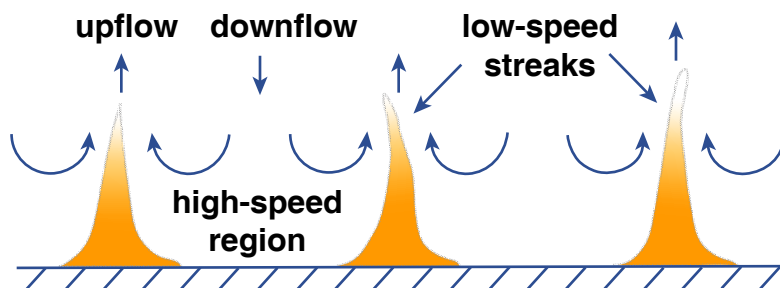


Figure by MIT OpenCourseWare.

Figure 4-40. Cartoon of low-speed wall streaks and intervening high-speed regions, as seen looking horizontally downstream near a horizontal wall. (From Smith, 1996.)

---

**156** The common visual manifestation of the burst–sweep cycle is the existence of streamwise-oriented *low-speed streaks* (also called wall-layer streaks, or just streaks) just above the flow boundary. These streaks are low-speed zones that lie between intervening high-speed zones. In the low-speed zones, slow-moving fluid has an upward (that is, in the direction away from the boundary) component of motion as a result of downward flow in the high-speed zones (Figures 4-39, 4-40). Sediment particles tend to be swept into the low-speed streaks as the faster-moving fluid in the high-speed zones moves slightly obliquely toward the low-speed zones.

**157** You might have seen such low-speed streaks on a cold winter day, with temperatures well below freezing, when a wind-driven light snow first falls upon a pavement, or in the desert when a strong wind blows fine sediments across the road surface. It is not difficult to set up a beautiful visual demonstration of low-speed streaks in a laboratory flume, where a small concentration of brilliant white sediment particles are transported across a dark-colored bare flume bottom.

**158** The strong message from such visualizations is that

- the streaks are strongly elongated parallel to the flow direction;
- the streaks waver and shift irregularly from side to side; and
- the streaks appear and disappear with time.

**159** Much effort has gone into study of the scale of the streaks. It is clear that for dynamically smooth flow the average spacing  $\lambda$  of the streaks, when nondimensionalized as  $\lambda^+ = \rho\lambda u_* / \mu$ , is in the range somewhat above or below 100, and only weakly dependent upon the mean-flow Reynolds number. The streaks are also present when the flow is dynamically fully rough; the spacing of the streaks, when nondimensionalized by dividing by the size of the close-packed roughness elements, is between 3 and 4. In transitionally rough flow, the situation is less straightforward.

**160** The burst–sweep cycle and its associated streak structure is a feature of the near-boundary part of the inner layer, in what was called in an earlier section the viscous sublayer (if one is present) and the buffer layer. Farther away from the boundary, where eddy scales range to larger size and where both production and dissipation of turbulent kinetic energy are less, there seems to be less coherence in the structure of the turbulence.

**161** It remains to look into how the counter-rotating vortices, stretched out in the streamwise direction, originate, and how their shapes evolve. It is generally accepted that the key features in this regard are vortices variously called *horseshoe vortices* or *hairpin vortices*, owing to their characteristic shape (Figures 4-41, 4-42). These vortices develop, in ways not yet well understood, and then become stretched downstream by the strong mean shear, and as they are stretched, the vorticity in the limbs increases. (In an approximate sense, as the diameter of the spinning fluid is decreased, the spinning is compressed into a smaller cross section, and the rate of spinning increases.) These elongated vortex limbs are generally believed to be responsible for the fluid motions in the burst–sweep cycle.

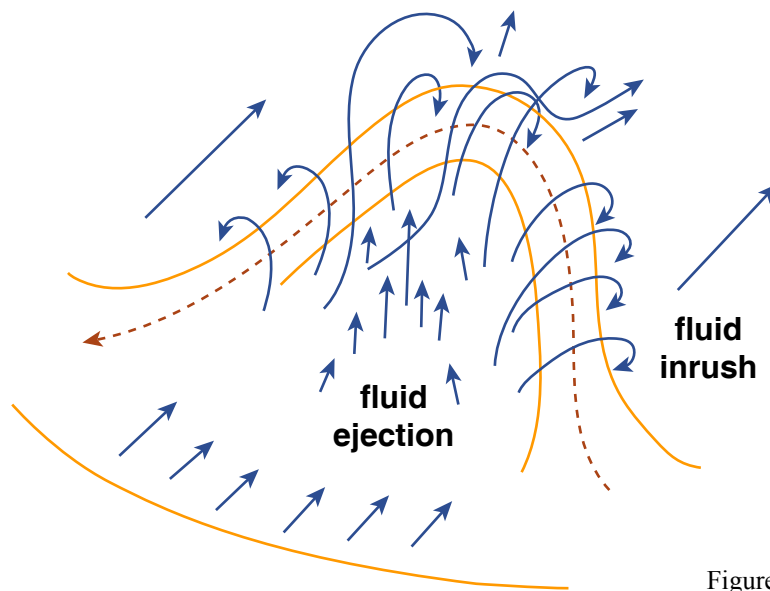


Figure by MIT OpenCourseWare.

Figure 4-41. Model of a near-wall horseshoe vortex. (Modified from Grass and Mansour-Tehrani, 1991; originally from Theodorsen, 1952.)

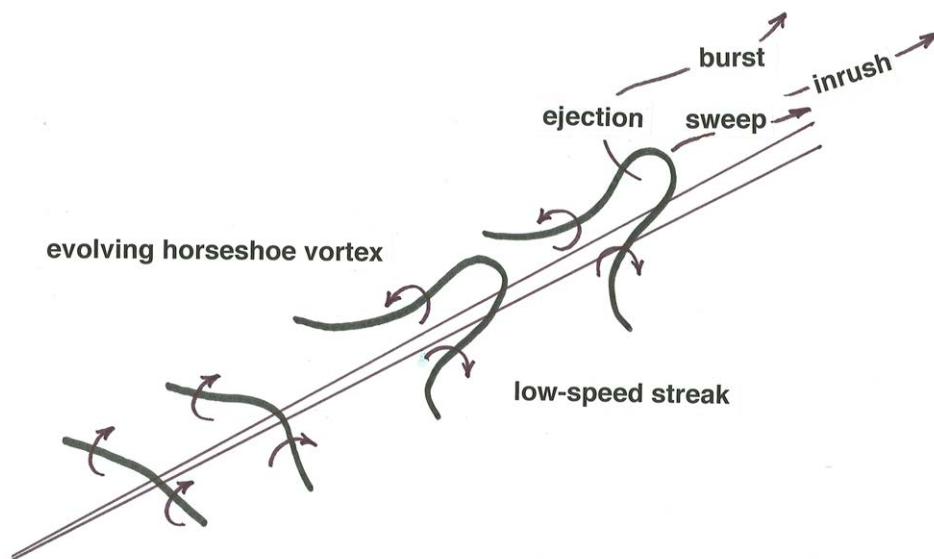


Figure 4-42. Formation and evolution of a horseshoe-hairpin vortex, showing its role in the burst-sweep cycle. (Modified from Hinze, 1975.)

**162** The study of coherent structures in turbulent shear flows is an active area of research. For informative reviews of the status of understanding, see Robinson (1991), Grass and Mansouri-Tehrani (1996), and Smith (1996). Also on the reading list at the end of the chapter are some of the classic papers: Kline et al. (1967), Corino and Brodkey (1969), Grass (1971), and Offen and Kline (1974, 1975).

---

***References cited:***

- Coleman, N.L., 1981, Velocity profiles with suspended sediment: *Journal of Hydraulic Research*, v. 19, p. 211-229.
- Corino, E.R., and Brodkey, R.S., 1969, A visual investigation of the wall region in turbulent flow: *Journal of Fluid Mechanics*, v. 37, p. 1-30.
- Grass, A.J., and Mansour-Tehrani, M, 1996, Generalized scaling of coherent bursting structures in the near-wall region of turbulent flow over smooth and rough boundaries, *in* Ashworth, P.J., Bennett, S.J., Best, J.L., and McLelland, S.J., *Coherent Flow Structures in Open Channels*: Wiley, p. 41-61
- Grass, A.J., 1971, Structural features of turbulent flow over smooth and rough boundaries: *Journal of Fluid Mechanics*, v. 50, p. 233-255.
- Grass, A.J., Stuart, R.J., and Mansour-Tehrani, M, 1991, Vortical structures and coherent motion in turbulent flow over smooth and rough boundaries: *Royal Society (London), Philosophical Transactions*, v. A336, p. 35-65.
- Hinze, J.O., 1975, *Turbulence*, Second Edition: McGraw-Hill, 790 p.
- Izakson, A., 1937, Formula for the velocity distribution near a wall [in Russian]: *Zhurnal' Eksperimental'noi i Teoreticheskoi Fiziki*, v. 7, p. 919-924.
- Kline, S.J., Reynolds, W.C., Schraub, F.A., and Runstadler, P.W., 1967, The structure of turbulent boundary layers: *Journal of Fluid Mechanics*, v. 95, p. 741-773.
- Millikan, C.B., 1939, A critical discussion of turbulent flow in channels and circular tubes: *Fifth International Congress on Applied Mechanics*, Cambridge, Massachusetts, Proceedings, p. 386-392.
- Monin, A.S., and Yaglom, A.M., 1971, *Statistical Fluid Mechanics*, Volume 1: Cambridge, Massachusetts, MIT Press, 769 p.

- Morris, H.M., 1955, Flow in rough conduits: American Society of Civil Engineers, Transactions, v. 120, p. 373-398.
- Nikuradse, J., 1933, Gesetzmässigkeiten der Turbulente Strömung in glatten Rohren: VDI Forschungsheft 356.
- Offen, G.R., and Kline, S.J., 1974, Combined dye-streak and hydrogen-bubble visual observations of a turbulent boundary layer: Journal of Fluid Mechanics, v. 62, p. 223-239.
- Offen, G.R., and Kline, S.J., 1975, A proposed model of the bursting process in turbulent boundary layers: Journal of Fluid Mechanics, v. 70, p. 209-228.
- Robinson, S.K., 1991, Coherent motions in the turbulent boundary layer: Annual Review of Fluid Mechanics, v. 23, p. 601-639.
- Smith, C.R., 1996, Coherent flow structures in smooth-wall turbulent boundary layers: facts, mechanisms and speculation, *in* Ashworth, P.J., Bennett, S.J., Best, J.L., and McLelland, S.J., Coherent Flow Structures in Open Channels: Wiley, p. 1-39.
- Tennekes, H., and Lumley, J.L., A First Course in Turbulence: Cambridge, Massachusetts, MIT Press, 300 p.
- Theodorsen, T., 1952, Mechanisms of Turbulence: 2nd Midwestern Conference on Fluid Mechanics, Ohio State University, Columbus, Ohio, Proceedings, p. 1-18.
- Tritton, D.J., Physical Fluid Dynamics, Second Edition: Oxford University Press, 519 p.